IJMMM International Journal of Minerals, Metallurgy and Materials 矿物冶金与材料学报（英文版）

A review of *in-situ* high-temperature characterizations for understanding the processes in metallurgical engineering

Yifan Zhao, Zhiyuan Li, Shijie Li, Weili Song, and Shuqiang Jiao

Cite this article as:
Yifan Zhao, Zhiyuan Li, Shijie Li, Weili Song, and Shuqiang Jiao, A review of *in-situ* high-temperature characterizations for understanding the processes in metallurgical engineering, *Int. J. Miner. Metall. Mater.*, 31(2024), No. 11, pp. 2327-2344. https://doi.org/10.1007/s12613-024-2891-y

View the article online at SpringerLink or IJMMM Webpage.

INTERNATIONAL JOURNAL OF
Minerals, Metallurgy and Materials

Volume 31, Number 11, November 2024
Page 2327

Review

https://doi.org/10.1007/s12613-024-2891-y

A review of *in-situ* high-temperature characterizations for understanding the processes in metallurgical engineering

Yifan Zhao[1)], *Zhiyuan Li*[1)], *Shijie Li*[1,2),✉], *Weili Song*[1),✉], *and Shuqiang Jiao*[2)]

1) Institute of Advanced Structure Technology, Beijing Institute of Technology, Beijing 100081, China
2) State Key Laboratory of Advanced Metallurgy, University of Science and Technology Beijing, Beijing 100083, China
(Received: 15 January 2024; revised: 20 March 2024; accepted: 21 March 2024)

Abstract: For the rational manipulation of the production quality of high-temperature metallurgical engineering, there are many challenges in understanding the processes involved because of the black box chemical/electrochemical reactors. To overcome this issue, various *in-situ* characterization methods have been recently developed to analyze the interactions between the composition, microstructure, and solid–liquid interface of high-temperature electrochemical electrodes and molten salts. In this review, recent progress of *in-situ* high-temperature characterization techniques is discussed to summarize the advances in understanding the processes in metallurgical engineering. *In-situ* high-temperature technologies and analytical methods mainly include synchrotron X-ray diffraction (s-XRD), laser scanning confocal microscopy, and X-ray computed microtomography (X-ray μ-CT), which are important platforms for analyzing the structure and morphology of the electrodes to reveal the complexity and variability of their interfaces. In addition, laser-induced breakdown spectroscopy, high-temperature Raman spectroscopy, and ultraviolet–visible absorption spectroscopy provide microscale characterizations of the composition and structure of molten salts. More importantly, the combination of X-ray μ-CT and s-XRD techniques enables the investigation of the chemical reaction mechanisms at the two-phase interface. Therefore, these *in-situ* methods are essential for analyzing the chemical/electrochemical kinetics of high-temperature reaction processes and establishing the theoretical principles for the efficient and stable operation of chemical/electrochemical metallurgical processes.

Keywords: *in-situ* characterization methods; high-temperature electrochemistry; electrodes; molten salts; interfacial reaction

1. Introduction

The extraction of metals or metal compounds from ores and other resources is known as metallurgy, and it is a fundamental process in many different industries. In the metallurgical process of transforming ore into metal or alloy, various characterization methods can be used to analyze the material transformation process, aiming to optimize the production process, improve product quality, reduce cost and energy consumption, and minimize pollution [1–4]. The smelting process parameters, product quality, and other factors are directly impacted by the physicochemical features of molten salts, mineral phase, metallic phase, and electrochemical electrodes. To efficiently control the metallurgical process and enhance productivity, the interplay between the physical and chemical characteristics of the mineral phase, metallic phase, electrochemical electrode, molten salt, and external variables, including temperature, pressure, and composition, needs to be comprehensively understood [5–6]. By utilizing diverse analytical methods, colleagues in the industry can conduct comprehensive investigations into the correlation between the composition, structure, and physicochemical properties of the mineral phase, metallic phase, and electrochemical electrode, facilitating the identification of the most suitable mineral phase, electrochemical electrode, and molten salt system for distinct smelting procedures [7–10]. The electrochemical reaction occurring at the contact between the electrode and the molten salt plays a critical role in connecting these two phases. Through the examination of the electrode reaction mechanism, the correlation between the alterations in the composition and structure of the two phases can be elucidated, consequently facilitating the establishment of a fundamental framework for the control and adjustment of process parameters.

The utilization of *in-situ* characterization methods (Fig. 1) in the field of metallurgy holds significant importance in the understanding and analysis of the dynamic phenomena that occur during metal smelting and refining operations. *In-situ* X-ray computer microtomography (X-ray μ-CT), laser scanning confocal microscopy (LSCM), and synchrotron X-ray diffraction (s-XRD) are used to characterize the structure and morphology of electrodes. Laser-induced breakdown spectroscopy (LIBS), ultraviolet–visible absorption spectroscopy (UV–Vis), and high-temperature Raman spectroscopy are used to characterize the composition and structure of the molten salts. X-ray μ-CT and s-XRD are used to characterize

✉ Corresponding authors: Weili Song E-mail: weilis@bit.edu.cn; Shijie Li E-mail: sli@ustb.edu.cn

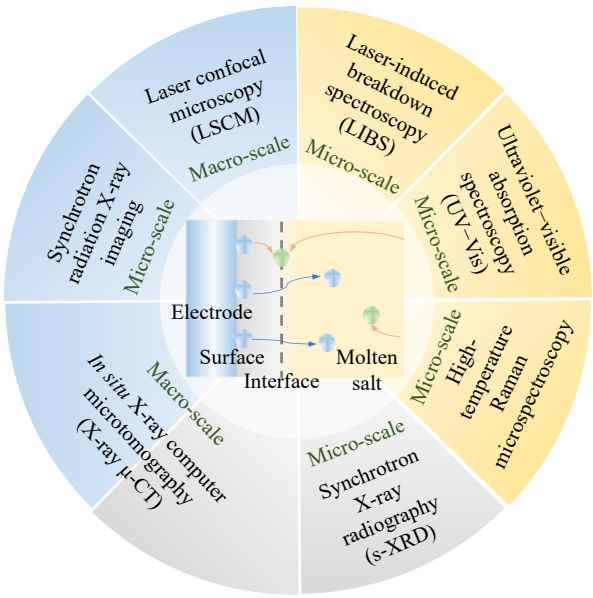

Fig. 1. High-temperature electrochemical characterization methods for characterizing electrode structures, molten salt compositions, and interfacial reactions.

the interfacial reaction mechanisms. These approaches facilitate the ability of scientists and engineers to observe and evaluate the behavior and transformations of materials in real time under the specific conditions of high temperature and reactive environments that are commonly encountered in metallurgical processes [11–12]. The electrode interface within the field of electrochemical metallurgy is a multifaceted and ever-changing barrier wherein reactions exhibit a high degree of sensitivity to certain factors, such as temperature, composition, and electric fields. The utilization of *in-situ* electrochemical techniques facilitates the comprehension of the reaction kinetics and mechanisms occurring at the electrode surface. The issue of the "confined black box" in the context of metal smelting pertains to the inherent complexity associated with the observation and regulation of the activities occurring within the smelting reactors. These processes typically lack transparency, making it arduous to employ conventional analysis techniques [13–17]. *In-situ* characterization methods, such as X-ray imaging and X-ray diffraction (XRD), enable the investigation and analysis of processes by providing insights into their internal mechanisms. These techniques enable a more comprehensive comprehension and management of these processes by unveiling previously inaccessible information. Through the examination of *in-situ* observations in conjunction with the characteristics and integrity of the outcome, colleagues in the industry can modify process parameters to enhance the efficacy of the product. In summary, the integration of sophisticated *in-situ* characterization methods into metallurgical processes holds immense value in enhancing our comprehension of material behavior under process conditions, optimizing metal production, elevating product quality, and attaining increased efficiency and stability in operations. These methods provide a means to gain insight into hitherto unexplored facets of smelting processes, hence facilitating enhanced decision-making and technological progress within the realm of metallurgy [18–22].

These methods enable the live monitoring and examination of substances in their authentic processing circumstances, which frequently involve severe factors such as temperature, pressure, and chemical reactivity. These approaches enable a more profound comprehension of the basic processes by providing insights into the dynamic changes occurring within materials during metallurgical procedures. In the domain of metal melting and smelting, the utilization of *in-situ* characterization techniques has played an essential role in elucidating the laws governing macrodynamic evolution and the mechanisms underlying reactions [23–24]. By incorporating these *in-situ* methods into multiscale research methods, scientists can establish connections between microscopic events and the resulting products of macroscopic processes [25–28]. Comprehensively understanding different perspectives is critical for optimizing the process parameters, enhancing material qualities, and advancing the development of new materials and processes. The utilization of these methods can yield valuable insights that can facilitate the creation of innovative materials possessing customized features and enhance the efficiency of production systems [29–32]. Therefore, *in-situ* characterization serves not only as a research tool but also as a catalyst for innovation and technological advancements in the fields of materials science and metallurgy. Therefore, the methodical incorporation and utilization of diverse *in-situ* characterization approaches in metallurgical processes play a significant role in the continuous advancement of materials research. These techniques provide unique benefits for the analysis and comprehension of intricate interactions inside materials, consequently enabling colleagues in the industry to expand the limits of materials design and process optimization.

2. Methods of solids analysis

2.1. Structural analysis

The XRD technique is highly effective in the examination of solid materials, providing valuable insights into their physical phase and crystal structure, and is extensively employed in the field of structural research. The present methodology encompasses the phenomenon of X-ray interaction with a given substance, including the X-rays to undergo scattering, absorption, or transmission within the material [33–34]. The phenomenon of diffraction can be observed when X-rays are scattered, resulting in the displacement of XRD lines. This displacement is determined by several factors, such as the form and dimensions of the crystal unit cell and the spacing between crystal surfaces. The determination of the relative intensity of diffraction lines is contingent upon the composition, quantity, and spatial configuration of atoms within the crystal lattice. Fundamentally, every crystalline material has an individualized structure, and the diffraction lines can be employed to ascertain the composition, crystal type, intramolecular bonding mechanism, molecular configuration,

and other properties of the substance. During materials analysis by XRD, the diffraction lines associated with the individual crystals can be employed to ascertain the composition of the substance [35–36]. Moreover, the principle of the three strongest peaks can be used to identify the phases of the substance present in the sample. In conclusion, XRD serves as a valuable method for the characterization of the structural features of solids, providing comprehensive insights into their crystal structure, composition, and phase characteristics.

XRD is a highly effective technique utilized in the examination of crystal structure and phase transitions [37]. XRD particularly exhibits exceptional proficiency in the real-time monitoring of structural alterations throughout diverse processes, such as high-temperature sintering. One significant benefit of XRD is its inherent resistance to temperature variations, making it suitable for investigating phenomena occurring at elevated temperatures [38]. Rasooli *et al.* [39] employed XRD as a methodological approach to examine the reaction kinetics between TiH_2 powder and a pure aluminum (Al) melt at various temperatures. The findings of their study indicated that the reaction rate is impacted by two primary factors, namely, the extent to which hydrogen atoms permeate the titanium (Ti) lattice and the chemical interaction between molten Al and Ti. Based on the results obtained, the authors identified three distinct temperature ranges that correlate with the reaction mechanism. In the temperature range of 973 to 1023 K, the primary driving force behind the reaction between Ti and molten Al within the Ti lattice is largely attributed to chemical processes. At temperatures ranging from 1023 to 1073 K, the reaction is subject to the combined influence of both diffusion and chemical processes. Ultimately, in the temperature range of 1073 to 1273 K, diffusion emerges as the predominant governing mechanism. In summary, the reaction processes observed within these temperature ranges can be sequentially characterized by the predominance of the chemical reaction, a mix of diffusion and chemical reaction, and diffusion alone.

The study conducted by Nikkhou *et al.* [40] focused on the intriguing investigation of mineral leaching through *in-situ* s-XRD examinations. To achieve this objective, Nikkhou and coworkers devised a clever flow-through cell configuration that facilitates uninterrupted observation of the phenomenon of dissolution/crystallization occurring during the solution–mineral interaction (Fig. 2). The flow-through cell design described herein encompasses a procedural sequence wherein the leaching solution is preheated within a designated solution reservoir. Subsequently, the warmed solution is propelled through a pliant tube, facilitating its flow over the mineral sample that has been positioned within the cuvette. The temperature of the cuvette is consistently regulated by a hot blower that is strategically positioned beneath the sample. Once the leaching solution has reacted with the mineral sample, the solution flows out of cuvette and is reintroduced into the designated solution reservoir, thus establishing a closed-loop system. The distinctive configuration of this system enables the ongoing acquisition of XRD patterns during the solution–mineral reaction, thereby permitting the live observation of the dissolution and crystallization process. Using the previously described experimental setup, Nikkhou and coworkers conducted a comprehensive investigation of the structural characteristics of galena. Specifically, they compared the diffraction spectra obtained at different pH levels. The s-XRD patterns obtained from the *in-situ* leaching process of galena have produced noteworthy results. They observed a consistent reduction in the intensity of galena peaks as the process unfolded, indicating a progressive dissolution of galena. Moreover, the observed phenomenon of the galena peak vanishing over a short duration of 14 min indicates an accelerated leaching rate under specific experimental parameters (Fig. 2(b)). This observation is consistent with a prior investigation that documented the rapid leaching of galena under comparable circumstances. The experimental conditions encompassed the utilization of a citric acid buffer solution maintained at a temperature of 308 K and a pH value of 6 while maintaining a flow rate of 0.5 $mL \cdot min^{-1}$. The s-XRD patterns of galena show a higher-than-expected intensity of the (200) peak at 11.4° (Fig. 2(c) and (d)). Therefore, the utilization of *in-situ* s-XRD investigations to observe and comprehend the real-time dissolution/crystallization process not only supports existing research findings but also significantly contributes to the domain of mineral leaching.

2.2. Morphological analysis

The laser scanning confocal microscope (LSCM) is widely recognized as a powerful instrument for morphological analysis. The system functions by employing a laser beam as an illuminating source, which is concentrated on the specimen and systematically traverses each location on the focal plane of the sample [41]. The detection of fluorescence released as a result of the excitation of the incident light path is accomplished by employing a photomultiplier tube when the tissue samples contain fluorescent chemicals. Data are subsequently analyzed by a computer system to render the visual representation. One notable feature of the LSCM is its capacity to deliver high-resolution three-dimensional (3D) imaging and noninvasive surface analysis, making it a suitable instrument for the examination of the surface topography and morphology of various materials. The LSCM can precisely depict the degree of roughness, texture, and outcomes of surface treatment [42]. The LSCM confers significant advantages in the study of surface evolution phenomena by enabling the *in-situ* observation of sample surfaces. The distinctive capacity of this tool renders it a valuable instrument for the examination of high-temperature processes, such as those involved in the production of steel. The LSCM can provide a 3D representation of the surface topography and morphology, providing scientists with insights into the dynamic changes occurring on the surface of a material over time and under various environmental circumstances. The acquisition of this information holds significant importance in the optimization of processes, such as steelmaking. By

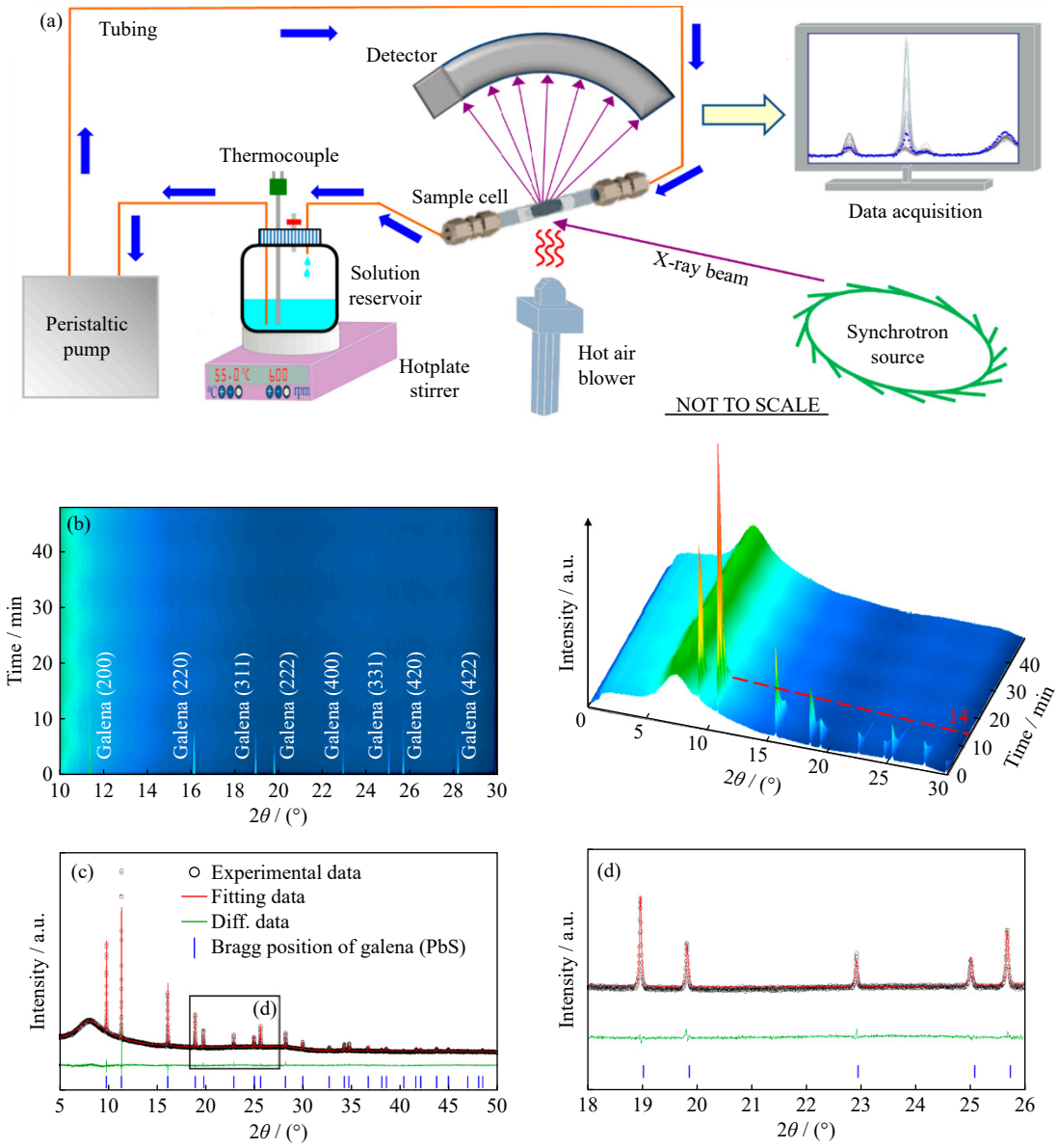

Fig. 2. Schematic diagram of the XRD setup and *in-situ* s-XRD images of the samples [40]: (a) schematic diagram of the flow-through cell experimental apparatus; (b) PXRD mapping of the *in-situ* leaching process of galena; (c, d) s-XRD patterns of galena.

comprehending the progression of the surface of the material, adjustments can be made to the process to improve the quality of the final product. Hence, the LSCM is not only a powerful tool for morphological analysis [43] but also an invaluable asset in industries where understanding material surface changes can lead to process optimization and product improvement.

High-temperature laser scanning confocal microscopy (HT-LSCM) has emerged as a tool of the comparable capability to the laser ultrasonic method, particularly in the aspects of heating and cooling rates and the speed of data acquisition. HT-LSCM has been proven to be an invaluable asset for the *in-situ* observation of solid materials, capturing the intricacies of microstructural transformations in real time. Fuchs and Bernhard [44] pioneered the use of HT-LSCM for the direct visualization of austenite grain growth, meticulously designing experimental setups tailored for real-time grain growth observations. Their work provided a critical evaluation of the factors influencing grain size measurement, such as the choice of materials and the operational specifics. They highlighted the profound impact of the research material on experimental outcomes and underscored the necessity of precise temperature control to ensure sample integrity, accounting for a potential temperature discrepancy of ±30 K between the target and actual surface temperatures. The introduction of an argon atmosphere is also noted as a strategic measure to prevent surface oxidation during experiments. Their findings affirmed that the grain growth visible on the surface of the sample is indicative of the bulk properties of the material. By accurately quantifying the average grain size and its distribution at various intervals, they established a robust foundation for validating models and simulations of grain growth, thereby cementing the status of HT-LSCM as a potent and dependable instrument for steel research applications.

In parallel, Liu and coworkers [45] employed LSCM to conduct *in-situ* examinations of the phase transformation dy-

namics in calcium-treated steel. They meticulously monitored the morphological evolution of inclusions transitioning from CaO–MgO–Al_2O_3 to CaO–MgO–Al_2O_3–CaS under experimental conditions. Their innovative approach involved LSCM to observe the transformation of Al_2O_3–CaO inclusions under various heating durations, using 3D imaging to unravel the underlying mechanisms of inclusion evolution during heating. Their observations revealed the gradual formation of a CaS layer enveloping the MgO–Al_2O_3 core of the inclusions, with the thickness of the layer proliferating over time. They also discovered that elevated heating temperatures catalyze elemental diffusion, facilitating the emergence of the CaS phase within the inclusions.

Moreover, Ren *et al.* [46] utilized LSCM to delve into the dissolution kinetics of Al_2O_3 in CaO–Al_2O_3–SiO_2 slag at high temperatures. By considering the impact of slag viscosity on inclusion dissolution, Ren and coworkers extracted the diffusion coefficients, applied the diffusion equation to decipher the dissolution mechanism, and pioneered a novel dissolution model. In another study, Yao and coworkers [47] harnessed the capabilities of LSCM to investigate the evolution of different ferrite forms in Ti-bearing high-strength, low-alloy steel. Their studies, as illustrated in Fig. 3, demonstrated that, with the austenitizing temperature increasing from 1523 to 1673 K, the volume fraction of acicular ferrites (AFs) notably increased from 17.6% to 23.2% in steel with 0.0070wt% Ti content. Conversely, in steel with a higher Ti content of 0.0370wt%, the volume fraction of AFs decreased from 78.7% to 52.5%. These variations in the volume fraction of AFs were observed to correlate with the initial temperature of the AF and ferrite side plate (FSP) phase transformations (Fig. 3(c)). For 70Ti steel with the austenitizing temperature of 1673 K, the FSP in the dashed box started to nucleate and grow at the crystal boundaries when the temperature was reduced to 1043 K. The AF started to nucleate at the surface of the inclusions when the temperature reduced to 983.8 K. At an austenitizing temperature of 1623 K, the AF transformation occurs at 976.5 K, and the FSP transformation occurs at 995.9 K. Their study outcomes also indicated a linear relationship between the Gibbs free energy and the austenite grain size during the AF phase transformation, providing deeper insight into the thermodynamic behavior of the material.

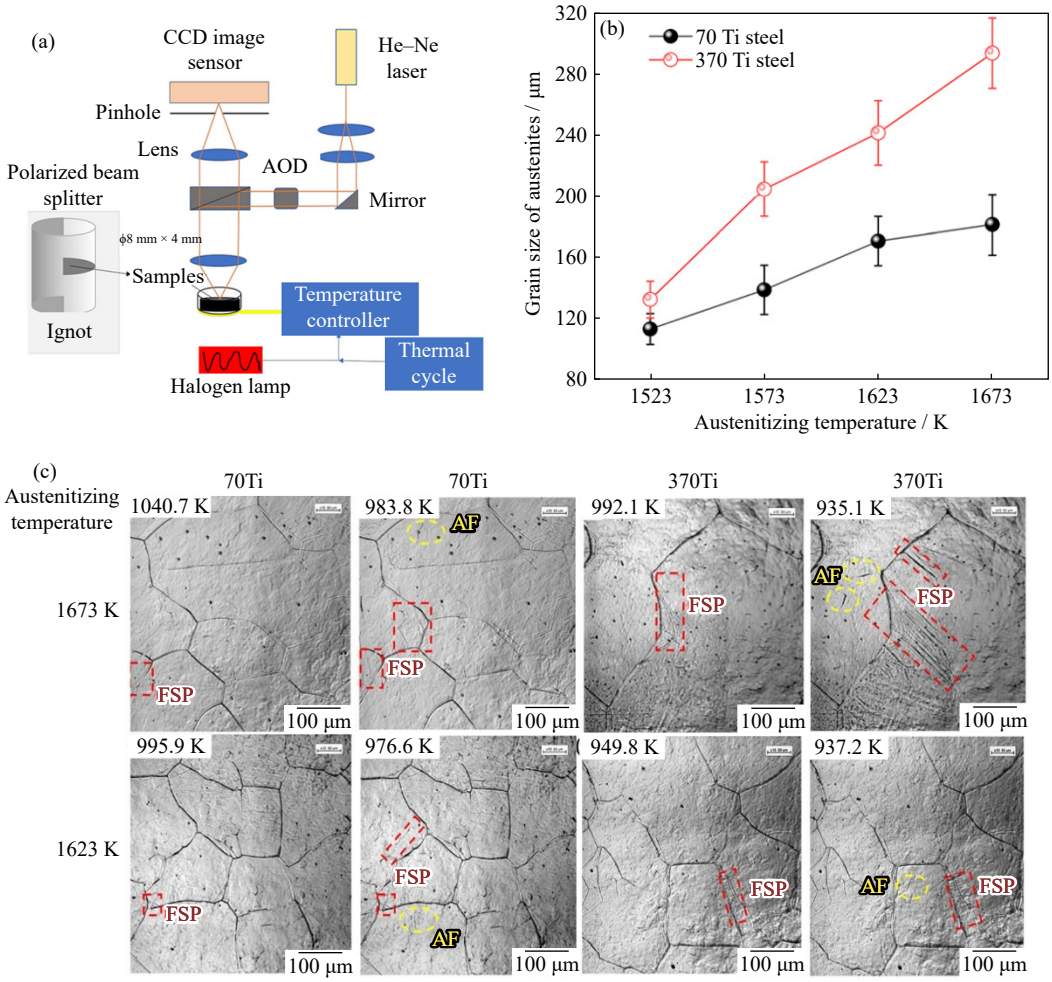

Fig. 3. Schematic of the HLSM device and *in-situ* HT-LSCM images of the sample [47]: (a) schematic representation of a sample processed and analyzed using the HLSM device; (b) relationship between austenite grain size and austenitizing temperature; (c) original HT-LSCM images of ferrite side plates (FSPs) and acicular ferrites (AFs) under different auscularizing temperatures. Reprinted by permission from Springer Nature: *Metall. Mater. Trans. B*, *In situ* observation and prediction of the transformation of acicular ferrites in Ti-containing HLSA steel, H. Yao, Q. Ren, W. Yang, *et al.*, Copyright 2022.

The application of X-ray μ-CT in high-temperature electrochemistry has indeed shown significant potential in addressing the challenges posed by harsh reaction conditions. X-ray imaging has emerged as an effective tool for the dynamic observation of the internal structure of opaque materials and for analyzing solid–liquid interfaces [48]. X-ray μ-CT confers nondestructive sampling and noncontact properties, making it suitable for integration with high-temperature electrochemical systems. X-ray μ-CT has been proven to be a powerful *in-situ* tool in materials science, providing intuitive and quantitative 3D imaging with high spatial resolution across multiple scales [49]. In the realm of room-temperature electrochemical systems, X-ray μ-CT has successfully monitored electrode evolution in lithium-ion batteries. In addition, in metallurgical electrochemistry, X-ray μ-CT can be used to probe the dynamic evolution of the 3D morphology and composition (four-dimensional (4D)) of electrodes, enabling the visualization of the complex 4D process through reconstructed images. The 4D analysis process based on X-ray μ-CT is characterized by multiscale visualization and high efficiency of data extraction, representing the profound integration of traditional electrochemistry and digital twin technology. This integration underscores the potential of X-ray μ-CT as a valuable technique for analyzing high-temperature electrochemical systems [50]. By providing insights into electrode dynamics and material evolution in these challenging environments, X-ray μ-CT can provide invaluable information that can be used to optimize these systems and improve their performance. Therefore, the use of X-ray μ-CT in high-temperature electrochemistry represents a significant advancement in the field.

The utilization of X-ray μ-CT in the field of high-temperature electrochemistry has demonstrated considerable promise in effectively addressing the difficulties encountered under severe reaction conditions. The utilization of X-ray imaging has become a prominent method for the dynamic examination of the internal composition of opaque materials, as well as for the investigation of interfaces between solid and liquid phases. One of the primary benefits of X-ray μ-CT lies in its nondestructive sampling and noncontact characteristics, rendering it compatible for integration with high-temperature electrochemical systems [51]. X-ray μ-CT has demonstrated significant efficacy as an *in-situ* instrument in the realm of materials research, having both intuitive and quantitative 3D imaging capabilities with exceptional spatial resolution across many scales. X-ray μ-CT has been proven to be an effective technique for monitoring the evolution of electrodes in lithium-ion batteries within the realm of room-temperature electrochemical systems. Moreover, in the field of metallurgical electrochemistry, X-ray μ-CT can investigate the dynamic evolution of the 3D morphology and composition (4D) of electrodes [52]. The utilization of reconstructed images facilitates the visualization of the intricate 4D process. The 4D analytical technique, which relies on X-ray μ-CT, is distinguished by its capability to visualize several scales and efficiently extract data. The aforementioned phenomenon exemplifies a significant amalgamation of conventional electrochemistry and digital twin technology [53−54]. The utilization of X-ray μ-CT in the investigation of high-temperature electrochemical systems highlights its considerable potential as a helpful analytical method. X-ray μ-CT can provide useful insights into the dynamics of electrodes and the evolution of materials inside demanding environments. This knowledge may be utilized to optimize these systems and enhance their overall performance. Hence, the utilization of X-ray μ-CT in the domain of high-temperature electrochemistry constitutes a noteworthy progression.

In-situ X-ray μ-CT is indeed a powerful technique that enables colleagues in the industry to explore the internal geometry and changes within materials under various conditions, including high temperatures and reactive environments [55]. The study conducted by Chen-Wiegart and coworkers [53] is an example of how *in-situ* 3D X-ray μ-CT can be used to gain insights into the dynamics of electrochemical processes, such as dealloying. Chen-Wiegart's use of *in-situ* 3D X-ray μ-CT to analyze dealloying in a heated molten salt environment helped visualize and understand the mechanism of the dealloying process. By observing the internal changes in the material as it interacts with the molten salt, Chen-Wiegart and coworkers identified the stages of dealloying, the rate at which it occurs, and the morphological changes that result from the process. Similarly, the study conducted by Chen-Wiegart and coworkers focused on real-time *in-situ* synchrotron 3D X-ray nano-stratigraphic imaging of molten salt dealloying, which provided valuable insights into the underlying mechanisms of the dealloying process. By achieving a high resolution at the nanoscale, this technique enabled Liu and coworkers to observe the formation of porous structures as the material underwent dealloying. This level of detail is important for understanding the kinetics and dynamics of the process. The implications of these studies extend beyond academic interest. The capability to tune the dealloying process and understand molten salt corrosion has important industrial applications, particularly in the fields of materials science, corrosion science, and electrochemistry. For instance, the insights gained can contribute to the development of advanced materials with controlled porosity and specific properties, which can be used in catalysis, energy storage, and structural applications. Moreover, the nontoxic and tunable nature of the dealloying techniques investigated using *in-situ* 3D X-ray μ-CT indicates that these methods could be environmentally friendly alternatives to traditional processes, which is particularly important in industries where toxic by-products or waste are a concern. Overall, the use of *in-situ* 3D X-ray μ-CT in high-temperature electrochemical research represents a significant step forward in the capability to analyze and understand complex material behavior under real-world conditions. This technique enables the acquisition of 3D data without destroying the sample, ensuring a more comprehensive understanding of material properties and processes.

The study conducted by Jiao and coworkers [56] served as

a notable illustration of the utilization of *in-situ* X-ray μ-CT for investigating high-temperature electrochemical phenomena (Fig. 4). Using this technique to investigate the electrolytic process under various conditions, they were able to capture real-time 3D images of the electrodes (Fig. 4(f) and (g)), which provided a unique and detailed perspective on the dynamic changes occurring within the electrodes during the electrochemical reactions. The capacity to detect these alterations in real time under various circumstances, including fluctuating current input forms, current densities, temperatures, and molten salt compositions, confers a notable advantage (Fig. 4(h) and (i)), enabling scientists to directly monitor and comprehend the influence of these parameters on the electrolytic process in high-temperature molten salts. This detail is important for optimizing these processes and improving the performance and efficiency of electrochemical systems. Moreover, the use of X-ray μ-CT to analyze the dynamic evolution of electrodes provides valuable information about the changes in electrode structure and chemical composition over time, which can provide insights into the internal mechanisms of electrochemical reactions under different electrolytic conditions. Comprehending these mechan-

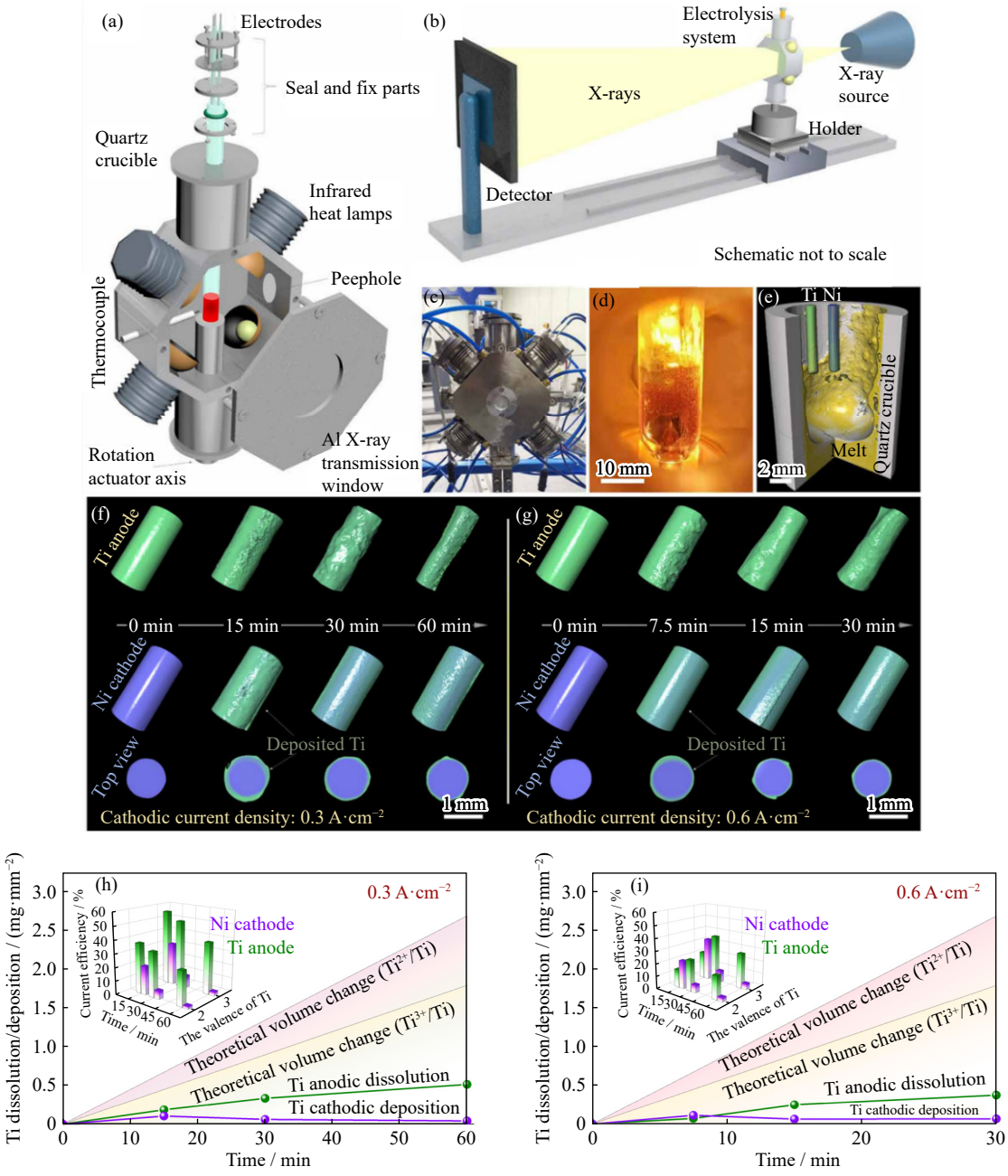

Fig. 4. 4D imaging apparatus for high-temperature electrochemistry: schematics and photographs [56]: (a) 3D schematic diagram of the assembled high-temperature electrochemical 4D characterization equipment; (b) schematic of the device in X-ray μ-CT transmission mode; (c) photograph of the 4D research equipment; (d) photograph of the high-temperature electrolyzer peephole; (e) 3D reconstructed image of the experimental electrolyzer at high temperature; (f, g) 3D reconstructed images of Ti anode and Ni cathode in different electrolysis time ranges at current densities of 0.3 A·cm^{-2} (f) and 0.6 A·cm^{-2} (g); (h, i) changes in Ti anode dissolution mass and Ti deposition mass in Ni cathode at different electrolysis stages.

isms is critical for the advancement of electrochemical systems in terms of efficacy and efficiency. In brief, the utilization of *in-situ* X-ray μ-CT in the field of high-temperature electrochemistry represents a robust methodology that can ensure a comprehensive understanding of the intricate phenomena occurring within such systems. The utilization of this methodology can considerably enhance our comprehension of electrochemical processes occurring at elevated temperatures, thereby making a valuable contribution toward the enhancement of electrochemical systems.

3. Molten salt analysis methods

3.1. Compositional analysis

The LIBS methodology has gained recognition as a reliable and adaptable analytical method because of its multitude of benefits. Due to the absence of sample preparation and the rapid response time, LIBS is ideal for a multitude of industrial applications, particularly those that necessitate real-time analysis [57]. In the context of the metallurgical industry, the utilization of LIBS has been observed as a viable method for conducting real-time investigation of the composition of steel and slag. The significance of this matter lies in the fact that the composition of these elements holds substantial sway over the characteristics exhibited by the end product. By employing LIBS, metallurgists can continuously monitor the compositions of materials in real time [58], enabling them to promptly make the necessary modifications to the manufacturing process, thereby guaranteeing the attainment of the highest possible level of product quality. In the context of alloy manufacture, LIBS can be effectively employed to assess the elemental composition of the alloy during the manufacturing procedure. Ensuring that the alloy has the desired qualities is of utmost importance. Through the real-time monitoring of the manufacturing process, manufacturers can make essential modifications to ensure the attainment of the required alloy composition. The LIBS technique has also demonstrated its suitability for environmental monitoring purposes. The capacity of LIBS to remotely detect and analyze several components concurrently endows it with significant utility as a tool for monitoring the quality of air, water, and soil, which can be particularly advantageous in regions where the potential hazard of pollution stemming from industrial operations exists. In general, the multifunctionality, rapidity, and noninvasive characteristics of LIBS render it a highly advantageous instrument in various fields of study [59]. The ongoing technological progress is expected to contribute to the expansion of the utilization of LIBS in both industrial and environmental contexts.

The studies undertaken by Gruber *et al.* [60−61] substantially contributed to showcasing the suitability and efficacy of LIBS inside the metallurgical sector and demonstrated the use of LIBS for monitoring elements, such as Cr, Cu, Mn, and Ni, in steel by focusing a laser beam on the surface of a molten specimen. This real-time monitoring can provide valuable insights into process control and quality assurance. Noll and coworkers [62−63] further demonstrated the versatility of LIBS by analyzing light elements, such as phosphorus, sulfur, and carbon, in molten steel and liquid slag samples. Their semi-online setup provided a practical example of how LIBS can be integrated into industrial processes. Zhang *et al.* [64] took a different approach by proposing an image-assisted method to address the issue of fluctuations caused by inconsistencies in the sample surface (Fig. 5). Their approach resulted in enhanced stability and precision of LIBS analysis, as evidenced by a notable decrease in the average relative standard deviations of intensity and projected concentrations of Cu, Mn, V, and Cr in the steel samples (Fig. 5(b)). The heights 1–20 (H1–20) are equivalent to 69.1 to 71 mm (in 0.1 mm increments) from lens 1 to the sample surface. In Fig. 5(b), H5 represents a height of 69.6 mm from lens 1 to the sample surface, while H15 represents a height of 70.5 mm from lens 1 to the sample surface. The *k*-values are one of 1–*p*, where *p* is the product of the mapped length and width of the original image matrix. Column 1 depicts the original image, while columns 2–4 illustrate the reconstructed images of H1 (b) and H15 (c) for varying *k* values (k = 50, 30, and 10). The aforementioned findings unequivocally indicate that LIBS has significant potential as a robust instrument for real-time compositional investigation in the metallurgical sector. The industry can considerably benefit from the capacity of this technology to provide real-time, precise, and consistent analysis of many elements concurrently, hence improving process control, quality assurance, and environmental monitoring. With the continuous advancement of technology, the utilization of LIBS in this particular domain would persistently broaden and undergo more development.

3.2. Structural analysis

The amalgamation of spectroscopic technology and electrochemical testing, commonly referred to as spectra electrochemical technology, is a noteworthy progression within the realms of analytical chemistry and materials research [65]. The utilization of hybrid technology combines the advantageous aspects of spectroscopy and electrochemistry, resulting in a more inclusive comprehension of chemical processes, specifically at the electrochemical interface. Spectroscopic methods, such as Raman spectroscopy, provide a means to obtain detailed information regarding the molecular structure and composition of materials characterized by high energy and resolution. When electrochemical testing with a high degree of sensitivity is utilized, colleagues in the industry can acquire electrical and optical signals simultaneously [66]. The utilization of a dual-signal methodology has been proven to be particularly advantageous in the investigation of reaction processes and the observation of transient species, including unstable intermediates. These species are frequently challenging to identify using conventional methods. The field of Raman spectroscopy has witnessed significant progress with the introduction of many techniques, including confocal, microscopic, and resonance Raman [67].

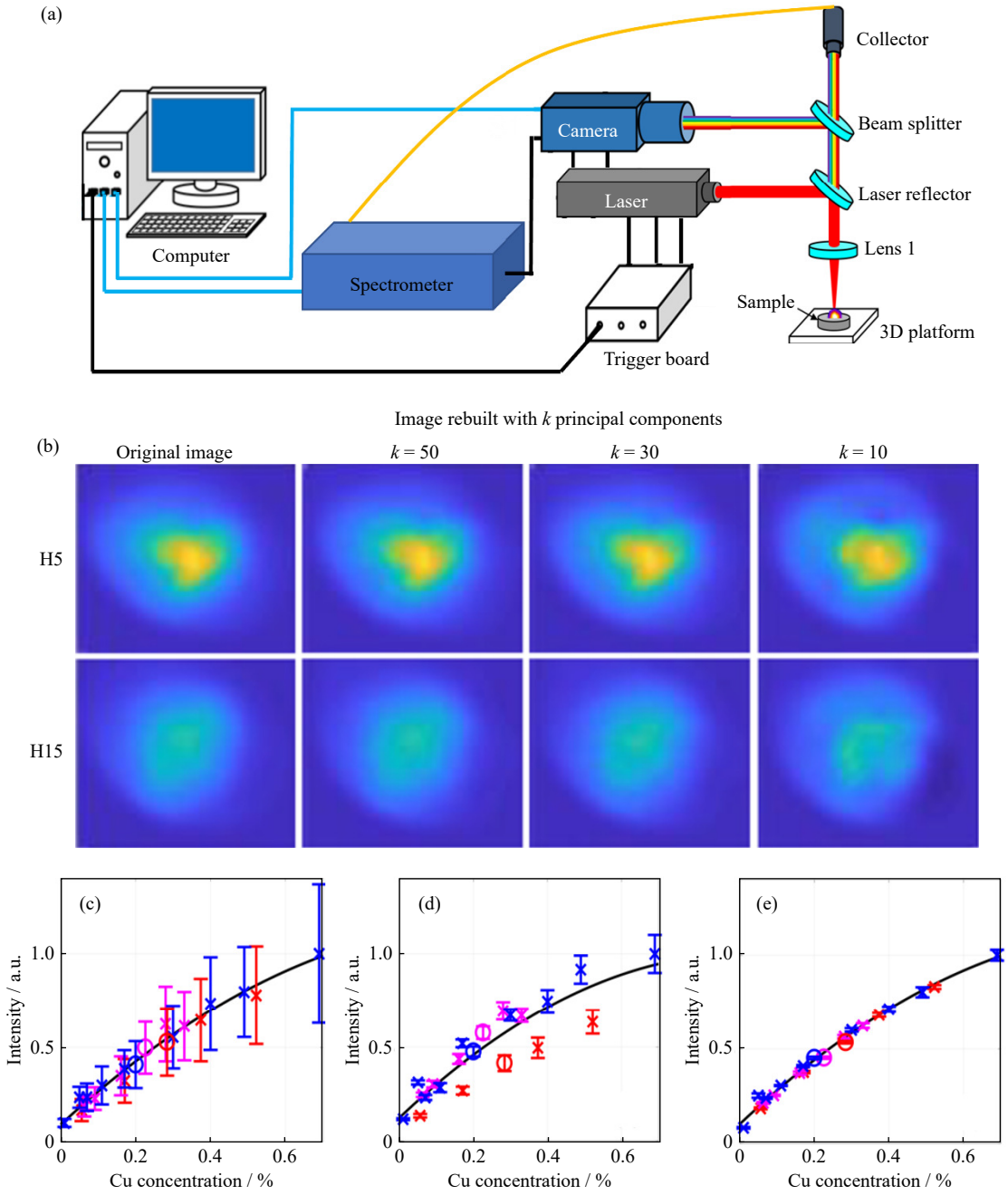

Fig. 5. Schematic image of the LIBS system and emission intensity images of the sample [64]: (a) schematic of the LIBS system; (b) the plasma launch intensity image of high-alloy steel; calibrations of Cu with the spectral line at 327.4 nm using (c) the original spectral intensity, (d) the entire spectral region normalization, and (e) the image-assisted method. Reprinted with permission from P. Zhang, L. Sun, H. Yu, *et al.*, *Anal. Chem.*, 90, 4686-4694 (2018) [64]. Copyright 2018 American Chemical Society.

These advancements have substantially enhanced the capacity to discern spatial and temporal intricacies at the molecular scale. The advancements observed can be mostly attributed to the utilization of improved detectors and higher-intensity lasers, hence augmenting the overall efficacy of Raman spectroscopy. Consequently, colleagues in the industry can examine the intricacies of electrochemical contacts with unparalleled accuracy, thereby enhancing the comprehension of reaction mechanisms and material characteristics. In the realm of molten salt electrochemistry, a comprehensive understanding of the structure and dynamics exhibited by molten salts is necessary. Molten salt electrolysis is a significant industrial procedure utilized for the extraction and purification of metals; meanwhile, molten salt batteries constitute a significant category of high-temperature energy storage technologies. The capacity to examine the configuration of molten salts facilitates the optimization of electrochemical processes, hence enhancing production efficiency and improving the performance of energy storage solutions. The examination of the composition and dynamics of molten salts can provide valuable knowledge that can be utilized in the formulation of novel electrochemical processes and the advancement of sophisticated materials [68]. The acquisition of this knowledge is of paramount importance in the pursuit of

enhancing the efficacy and sustainability of processes such as metal fabrication and augmenting the performance and safety of high-temperature battery systems. With ongoing research and technological improvements, the contributions of spectroscopy to electrochemical technology will continue to play a pivotal role in advancing our understanding and capabilities in these important areas [69–71].

The study conducted by Ma *et al.* [72] emphasized the potential of *in-situ* Raman spectroscopy in the analysis of microstructures in molten salt systems and the real-time monitoring of electrochemical events. In their study, Ma and coworkers employed *in-situ* high-temperature Raman spectroscopy to examine the microstructure of a molten K_3AlF_6–Al_2O_3 system. Their investigation was conducted in an argon environment, including a wide temperature span ranging from ambient temperature to 1273 K. Ma and coworkers augmented their experimental methodology by incorporating quantum chemistry *ab initio* simulations to forecast the vibrational wave numbers of prospective clusters inside the molten salt system. Through a comparative analysis between the computed outcomes and the empirical Raman spectra, Ma and coworkers successfully discerned the existence of diverse clusters, namely, $[AlF_5]^{2-}$, $[AlF_6]^{3-}$, $[Al_2OF_6]^{2-}$, and $[Al_2O_2F_4]^{2-}$. The utilization of a blend of experimental and computational techniques presents a potent means of investigating the microstructure of molten salt systems and comprehending their dynamics under elevated temperatures. Hu *et al.* [73] investigated the solubility of CO_2 in Li_2O–LiCl at Li_2O concentrations of 4wt%–8wt% Li_2O by Raman spectroscopy at 873–973 K and 101.3 kPa CO_2 using Li_2SO_4 as an external standard. Their results showed that the solubility of CO_2 increased with the increase in Li_2O concentration, reaching a maximum at 923 K and 8wt% Li_2O, with 0.1105 g CO_2 dissolved in 1 g melt and a conversion of Li_2O to Li_2CO_3 of 94.19%. Zhang *et al.* [74] examined the impact of temperature on the phosphorus distribution ratio and phosphate capacity, using Raman and MAS-nuclear magnetic resonance (NMR) techniques to characterize the structures. They observed that as the temperature increased from 1823 to 1873 K, the stability of the silicate and phosphate networks was compromised because of the weakening of the Si–O–Ca–O–P links, which led to a decrease in both the phosphorus distribution ratio and phosphate capacity. In addition, they determined that the mixing entropy of the dephosphorylation reaction at 1873 K was slightly higher than that at 1823 K, indicating a reversal of the dephosphorylation reaction with the increase in temperature.

The study undertaken by Jiao *et al.* [75] is a significant and noteworthy contribution to the field of high-temperature electrochemical investigation. The emergence of a novel electrochemical apparatus capable of integrating Raman spectroscopy analysis with optical microscopy imaging signifies a significant advancement in technology (Fig. 6). This innovation facilitates the comprehensive examination and evaluation of electrochemical phenomena occurring under high-temperature conditions. The capacity to conduct multi-dimensional operational analysis holds significant importance in the context of intricate systems, such as the reduction of high-valent Ti ions and the nucleation and development of Ti atoms during electrodeposition in molten salts (Fig. 6(b)). Through the integration of multivariate experimental studies and theoretical calculations, Jiao and coworkers successfully deconstructed the complex multistep reduction process at a temperature of 823 K (Fig. 6(c)). This endeavor holds significant importance in comprehending and enhancing high-temperature electrochemical processes. The capability of the instrument to monitor and regulate in real time enhances the understanding of the kinetics involved in the electrodeposition process. The aforementioned matter needs to be considered in the context of multivalent metals, such as Ti. The behavior of these metals in molten salt environments can be intricate because of their capability to exist in numerous oxidation states and the possibility of the formation of diverse intermediate species. Furthermore, the investigation into the influence of a magnetic field on the Ti electrodeposition process and the elucidation of the underlying scale-spanning mechanism is a significant step forward. Understanding how magnetic fields can regulate such processes opens up new possibilities for controlling and enhancing electrochemical reactions, potentially leading to more efficient and precise deposition techniques. The successful application of this instrument and the multidimensional analysis strategy not only validates the approach but also sets a precedent for future research in high-temperature electrochemistry. The insights gained from this work have substantial implications for a wide range of applications, including metal extraction, refining, and advanced material synthesis. In general, the contributions of Jiao and coworkers have established a powerful method for the in-depth analysis of high-temperature electrochemical systems. This method can provide valuable insights into the behavior of multivalent metals in molten salt environments, which can be leveraged to improve industrial processes and develop new technologies.

The UV–Vis absorption spectroscopy is of paramount importance when examining the electronic structure and coordination environment of metallic ions within molten salt systems [76]. The examination of valence electron behavior during photon absorption yields significant insights into the characteristics of chemical entities within a given system, including their electronic states and intermolecular interactions. The UV–Vis absorption spectra of molten salt systems are predominantly affected by ligand field transitions and charge transfer transitions [77]. The metallic ions present in these systems typically form associations with inorganic ions and are coordinated by anionic ligands as a result of electrostatic interactions. The coordination of transition metals with anionic ligands can result in the splitting of energy levels, a phenomenon that is caused by the presence of an electric field. The degree of energy level splitting is contingent upon the characteristics of the coordinating field [78]. As a result, the energy necessary for the absorption of photons by these divided energy levels also exhibits variation, hence produ-

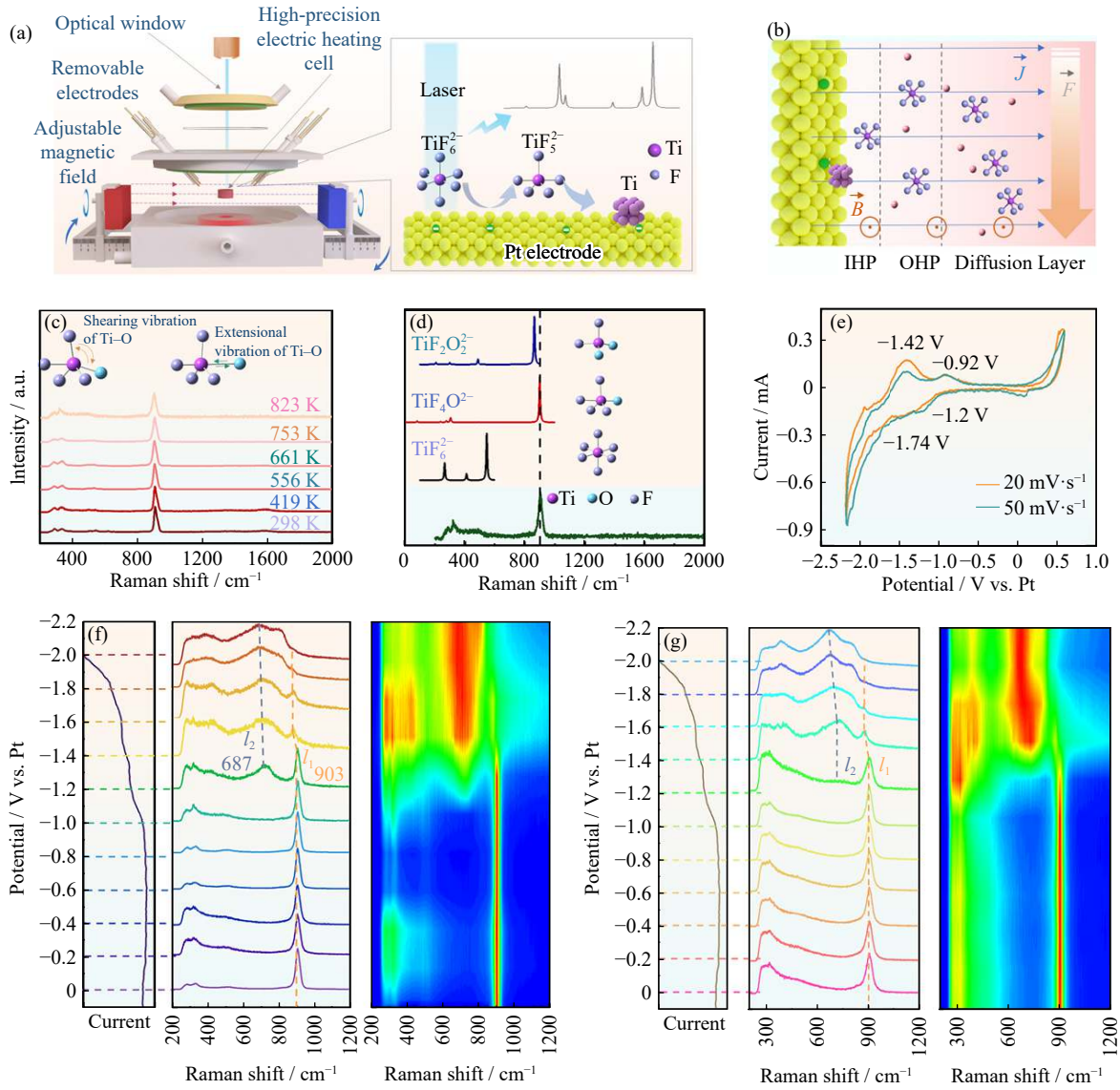

Fig. 6. Schematic diagram of high-temperature electrochemical multifunction operation analysis instruments [75]: (a) *in-situ* Raman probe, multi-price metal molten salt electrolyte optical microscope imaging, and cathode process electromagnetic adjustment equipment schematic diagram; (b) diagram of the electrode process used to regulate the magnetic field ($\vec{B}$, $\vec{J}$, and $\vec{F}$ are the magnetic field, current, and Lorentz force); (c) Raman spectra and Ti–O vibration mode (illustration) of the Pt electrode and the molten salt interface during the heating process; (d) theoretical Raman spectra of TiF_6^{2-}, TiF_4O^{2-}, and $TiF_2O_2^{2-}$ and the Raman spectrum of the interface between the Pt electrode and the molten salt at 823 K; (e) the cyclic voltammograms of Pt electrode in molten NaF–KFLiF–K_2TiF_6 at 823 K; (f) during the electrolytic process from 0 to −2 V, compared with Pt, the Raman spectra of the interface between the Pt electrode and molten salt; (g) Raman spectra that change with the electrode–molten salt interface in the magnetic field.

cing distinct absorption spectra. Through the examination of these spectra, the valence states and coordination configurations of the transition metal ions present in the molten salts can be ascertained. The capability to investigate the electronic structure and coordination environment of metallic ions in molten salt systems holds significant importance in several fields of academic inquiry and industrial applications, including materials science, metallurgy, and electrochemistry [79−80]. Analyzing the behavior of these systems under various settings can facilitate comprehension, property prediction, and performance optimization for many applications. Hence, UV–Vis absorption spectroscopy has emerged as an essential methodology in the investigation of molten salt systems, providing a substantial amount of data that can substantially enhance our comprehension of these intricate systems.

The studies conducted by T.J. Kim *et al.* [81] and B.Y. Kim and Yun [82] demonstrate the efficacy of combining high-temperature UV–Visible absorption spectroscopy with electrochemical techniques for investigating the behavior of ions in molten salt systems. T.J. Kim *et al.* [81] examined the redox characteristics of europium ions (Eu^{2+} and Eu^{3+}) within molten LiCl–KCl eutectic salts at elevated temperatures. Their study represents a noteworthy advancement in comprehending the intricate chemical behavior of f-block elements in such settings. The acquisition of knowledge regarding the

generation of EuOCl in the presence of oxygen ions and the subsequent evaluation of its solubility product under said circumstances hold significant importance for researchers and professionals in the field of molten salts. This knowledge is particularly relevant in the nuclear industry, where europium can serve as a fission product during the reprocessing of spent nuclear fuel. By contrast, B.Y. Kim *et al.* [82] not only provided support for the redox behavior of europium ions (Eu^{2+} and Eu^{3+}) at elevated temperatures but also enhanced comprehension by integrating time-resolved fluorescence spectroscopy. This methodology enabled the investigation of the kinetics of redox reactions and the impact of concentration on the reduction process of Eu^{3+} to Eu^{2+}. The examination of the interplay of the reduction ratio, the concentration of Eu^{3+} ions, and formal reduction potential under temperature fluctuations provides a more profound understanding of the thermodynamics and kinetics associated with the redox process in molten salt systems. Both papers demonstrated the application of sophisticated spectroscopic techniques at high temperatures for obtaining quantitative information on the speciation and redox chemistry of metal ions in molten salts. The acquisition of a large amount of data is of utmost importance in the advancement of effective methods for the retrieval of metals, the practice of recycling, and the management of waste in industrial settings characterized by elevated temperatures. The capacity to make accurate measurements under elevated temperatures presents novel opportunities for exploring not only europium but also other metal ions under comparable settings. The acquisition of knowledge obtained from these research studies is vital to the optimization of electrochemical processes, including those employed in the extraction and purification of metals, and to the advancement of our comprehension of chemical systems operating at high temperatures.

Liu *et al.* [76] meticulously developed a high-temperature *in-situ* UV–Vis absorption spectroscopy system, ensuring that the molten salt remains under an inert argon shield throughout the entire experimental sequence. This sophisticated setup ensured the precise analysis of the absorption spectra, enabling the identification of metal ion valences within the molten salt. Moreover, the setup facilitated real-time tracking of ion concentration fluctuations amid chemical reactions, providing insights into the underlying reaction mechanisms within the salt matrix. Their study delved into the intricate reaction dynamics between metallic Cr and Cr^{3+} ions in molten FLiNaK (LiF : NaF : KF molar ratio of 46.5:11.5:42) and FLiBe (LiF : BeF_2 molar ratio of 66.6:33.3) salts.The distinctive absorption peak at 450 nm serves as a reliable marker for differentiating between Cr^{2+} and Cr^{3+} ions in FLiBe salt, revealing that metallic Cr reacts with Cr^{3+} ions to yield Cr^{2+} ions. Furthermore, the study illustrates the intriguing behavior of Cr^{2+} ions in molten FLiNaK, which engage in disproportionation reactions leading to the reformation of both metallic Cr and Cr^{3+} ions, with Cr^{3+} ions persistently interacting with metallic Cr.

Furthermore, NMR can be utilized for the structural analysis of high-temperature inorganic molten salts and room-temperature ionic liquids. Bessada and Anghel [83] utilized a novel high-temperature, high-resolution solid-state NMR technique to analyze the structural properties of the $Na_2B_4O_7$–Na_3AlF_6 binary system across different states, ranging from a solid state at room temperature to a liquid state at 1373 K. The evolution of the ^{27}Al, ^{23}Na, ^{11}B, and ^{19}F NMR spectra with varying composition illustrates the integration of Al into $Na_2B_4O_7$ as both an $[AlO_4]$ and a sparse $[AlF_6]$ component within a vitreous framework and the generation of $[BOF_2]$ clusters leading to the formation of cured blends.

4. Interfacial reactions

4.1. Electrode dissolution/deposition

The achievement of uniform and stable products during the electrolytic process is a fundamental concern in the field of industrial metallurgical investigation. Therefore, electrochemical deposition needs to be regulated to inhibit the formation and growth of dendrites. The study conducted by Cui *et al.* [84] comprehensively examined the electrodeposition process at 298 K, with a specific focus on zinc deposition on planar electrodes. Through the utilization of *in-situ* observation via optical microscopy, their study significantly contributed to our understanding of the underlying dynamics of this process and provided insights into strategies for achieving homogeneity and stability in the resulting products. Their findings indicated that the process of zinc electrodeposition may be categorized into two distinct regions, namely, homogeneous and nonhomogeneous. Cui and coworkers proposed that the uniform deposition of zinc in the homogeneous zone can be extended by augmenting both the charging current and the viscosity of the electrolyte. This observation is important as it provides a way to control the deposition process to inhibit the formation and growth of dendrites, which can adversely affect the performance and safety of electrochemical devices, such as batteries. Their proposed mechanism for this behavior is quite interesting, i.e., a high charging current provides sufficient electrons for the deposition to occur beyond the deposition tip, leading to a more uniform deposition. Alternatively, an increase in the viscosity of the electrolyte hinders the transfer of ions, making the effect of distance more pronounced and thereby favoring uniform deposition. The study confers a potential pathway for enhancing the electrochemical deposition procedure in industrial metallurgical contexts. The manipulation of charging current and electrolyte viscosity can effectively control the deposition process, leading to the generation of products that exhibit enhanced uniformity and stability. The potential ramifications of this development extend to numerous sectors, including production, electroplating, and metal reclamation, among others.

X-ray μ-CT was employed by Jiao *et al.* [85] to visualize the electrorefining process of Ti (Fig. 7). Their results showed that the dissolution efficiency of pulsed electrolysis for the Ti anode and the thickness of the cathode layer were markedly improved compared with those observed for the Ti

anode under direct current (DC) electrolysis at the same current density (Fig. 7(c)). In addition, Jiao and coworkers showed that the current efficiency of pulsed electrolysis tends to increase when the current density decreases within the specified range of 0.1–0.4 A·cm^{-2}. More importantly, Jiao and coworkers employed numerical simulation techniques to monitor the variations in Ti ion concentration at the specific interface of the electrode. They observed that the concentration of Ti ions exhibited a continuous elevation on the surface of the cathode throughout pulsed electrolysis in contrast

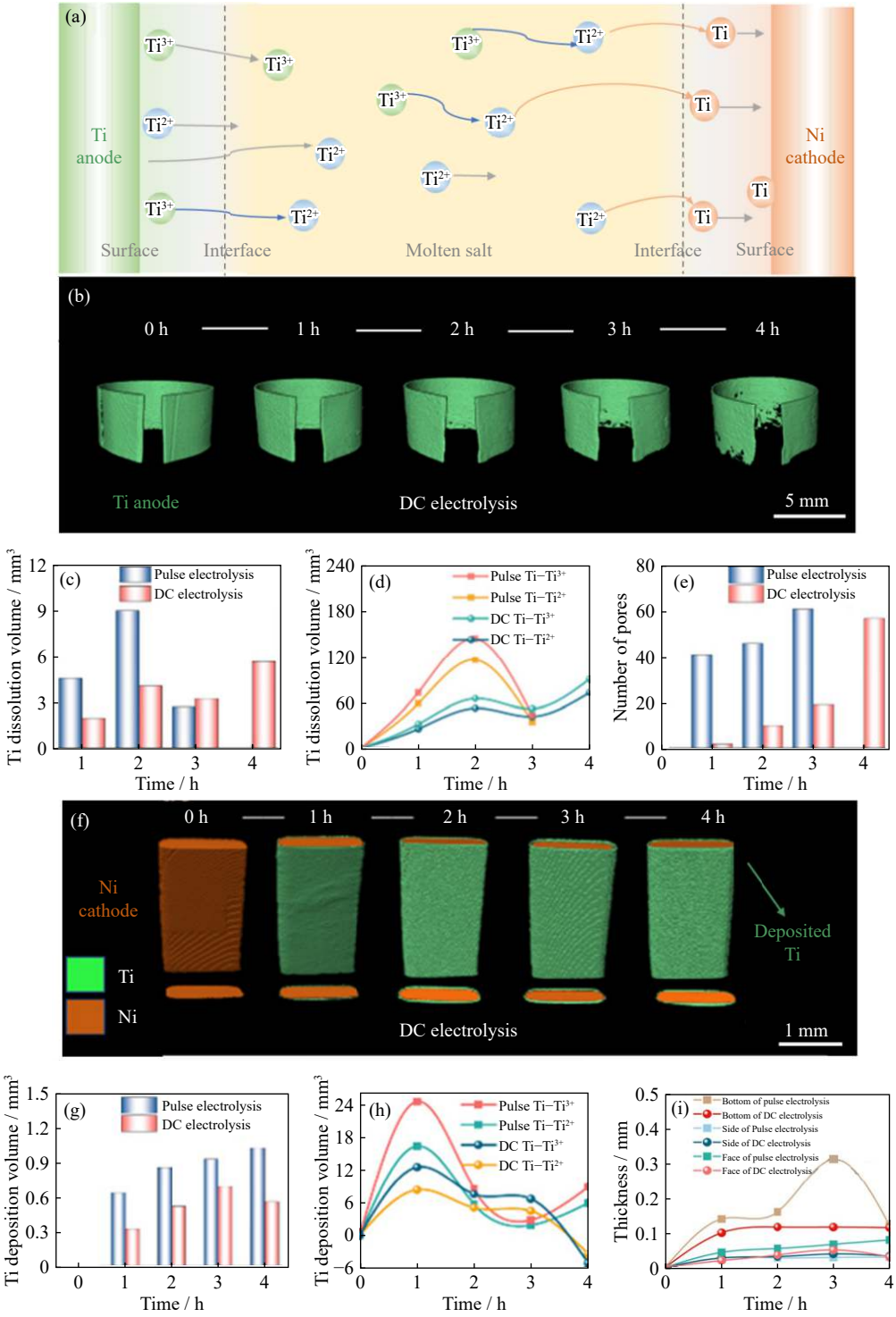

Fig. 7. (a) Schematic of the electrode reaction between the Ti anode and the Ni cathode. (b–i) 4D imaging and analysis of cathodic and anodic electrolytic processes in molten salts [85]: (b) Ti anode rendered in 3D; (c) volume change of the Ti anode; (d) conversion efficiency of the Ti anode; (e) number of dissolution vacancies in the Ti anode; (f) effect of DC electroplating on the cathode; (g) volume of Ti deposited on the cathode; (h) conversion efficiency of the Ni cathode; (i) deposit thickness of different parts of the cathode under pulsed and DC plating. (b–i) Used with permission of Royal Society of Chemistry, from Dynamic evolution of high-temperature molten salt electrolysis of titanium under different operational conditions, H.D. Jiao, M.J. Liu, Y. Gao, *et al.*, 10, 2023; permission conveyed through Copyright Clearance Center, Inc.

to DC electrolysis. Their study provided important perspectives on the occurrence of side reactions at the electrode interface, a critical aspect for enhancing the stability of Ti electrorefining processes. The study conducted by Jiao and coworkers has made advancements in the domain of industrial metallurgy, specifically in the area of controlling electrochemical deposition and comprehending the electrodeposition process.

4.2. Electrode gas production

The existence of gas bubbles during the electrolytic process can have a substantial effect on both the efficiency and stability of the process. As the bubbles migrate toward the unobstructed surface, they induce circulation and convection within the electrolyte, which can impact the distribution of electric current and result in fluctuations at the interface of the electrolyte. Furthermore, the presence of gas bubbles beneath the anode can result in elevated tank voltage and increased energy consumption. To mitigate the impact of gas bubbles on the electrolytic process, Fortin and coworkers [86] developed an aqueous solution model to simulate a 150 kA prebake Al electrolyzer. They analyzed the effects of various parameters, such as current density, pole pitch, anode tilt, and electrolyte flow rate, on the dynamics of the gas layer. The findings of their extensive investigation indicated that the pole pitch does not influence the behavior of gas. However, an augmentation in current density leads to the formation of larger bubbles, a thicker front of bubbles, an increased gas distribution across the anode region, and a higher velocity of bubble movement. Notably, the frequency of gas emission exhibited no changes in response to differences in current density. Alternatively, an increased flow rate of electrolyte results in a reduction in the size of bubbles and the extent of gas coverage on the anode region. However, it leads to an elevation in both the velocity of bubbles and the frequency of gas release. The modification of the anode tilt has an impact on the gas dynamics, resulting in the formation of reduced bubble sizes, decreased gas coverage, and increased frequency of gas release. Nevertheless, the angle of inclination does not have any effect on the velocity of the flow of the bubbles. The study undertaken by Fortin and coworkers significantly contributed to our understanding of the dynamics exhibited by gas bubbles in the context of electrolysis. Their study identified essential factors to be considered in the optimization of processes to minimize energy usage and improve overall efficiency.

Zhao *et al.* [87] utilized a laboratory-scale transparent Al electrolyzer to observe the bubble dynamics directly beneath the anode in an industrial electrolysis setting, marking the first instance of such observation. They also conducted measurements of corresponding cell voltages to quantitatively analyze their relationship with bubble kinetics. Their findings indicated that, as the current density increases, bubbles form at multiple points, and their quantity increases. Once the bubbles reach a certain size and the surface nears the edge of the anode, they swiftly escape from the bottom. Moreover, as the current density increases, the frequency of bubble release increases, whereas the bubble size decreases. The studies conducted by Utigard and coworkers [88] enhanced the comprehension of the intricate mechanisms underlying gas bubble dynamics in electrolytic processes. Their studies specifically concentrated on elucidating the characteristics and actions of hydrogen bubbles within the framework of liquid metal and solid interconnects. The aforementioned findings hold significant importance for businesses that heavily depend on electrolysis, such as Al manufacturing and the electrorefining of metals. The studies conducted by Utigard and Toguri pertaining to the behavior of gas bubbles at the anode during the electrolytic process significantly contributed to the understanding of the operational properties of electrolytic cells. The utilization of X-ray imaging facilitated the acquisition of distinct visual representations pertaining to the production and dynamics of bubbles, which would otherwise be challenging to discern. Notably, during typical electrolytic conditions, the anode side exhibits a multitude of small bubbles, whereas the lower region of the anode exhibits fewer but larger bubbles. The observed variation in bubble size and distribution can be ascribed to the heterogeneous conditions present on the anode surface and bottom, which encompass different factors, such as current density, electrolyte composition, and gas evolution dynamics. The anode effect, which was extensively investigated by Utigard and Toguri, is a notable disturbance observed in the electrolytic process. During the occurrence of the anode effect, the anode loses its capability to be wetted by the electrolyte. This phenomenon results in the development of a coherent layer of gas bubbles, which can expand to a thickness of up to 5 mm. The presence of a bubble layer serves as an insulating barrier, resulting in the elevation of electrical resistance. Consequently, this phenomenon can lead to fluctuations in cell voltage, thereby decreasing the overall efficiency and even causing harm to the cell. The observed results indicate a positive correlation with the concentration of alumina and current density, as well as a position correlation with the surface area of the bubbles and a negative correlation with the surface area of the bubbles and a negative correlation with the size of the bubbles. These findings hold significant implications for the optimization of the electrolytic process. By comprehending the impact of these parameters on the behavior of gas bubbles, operators can modify the electrolysis settings to reduce the production of sizable bubbles and the incidence of the anode effect, which, in turn, enhances the efficiency and stability of the process. The study conducted by Ding and coworkers [89] complements these findings by examining the evolution of hydrogen bubbles in liquid metal and solid interconnects, which is another aspect of gas behavior in electrolytic systems. Their study addressed the nucleation, growth, and detachment of hydrogen bubbles, which are critical factors in the design and operation of cells for processes such as water electrolysis for hydrogen production. Together, the aforementioned studies contribute to the body of knowledge necessary for the development of more efficient and ef-

fective electrolytic processes, with applications ranging from metal production to the generation of hydrogen as a clean energy carrier.

Ding and coworkers [89] conducted a pioneering study wherein they employed synchrotron X-ray imaging to perform *in-situ* observation of the progression of hydrogen bubbles within liquid Al/solid Ni interconnects. Their findings revealed that, during the heating process, individual bubbles primarily exhibit random growth patterns. The evolution of hydrogen bubbles during the heating process in the liquid Al/solid Ni interconnects is fascinating. At the onset, no hydrogen bubbles are observed. However, a significant number of spherical bubbles form in the liquid Al, reaching a peak at 960.1 K after 12.5 s. Concurrently, the interface between the two phases remains smooth, demonstrating that the liquid Al maintains a strong bond with the Ni substrate. As the temperature continues to increase, the number of bubbles initially increases rapidly, subsequently decreases gradually, and ultimately vanishes at the 117.5-s mark. This intriguing bubble behavior within the liquid Al and the Ni substrate is further described in detail. Three distinct types of bubble behavior were observed: (1) the majority of the bubbles grew to their maximum size before contracting and disappearing; (2) some bubbles initially grew, only to abruptly rupture; (3) a few bubbles transformed from a spherical shape to an ellipsoidal shape, gradually growing before rupturing. The aforementioned studies provide critical insights into the behavior of gas bubbles in various electrolytic processes and shed light on the underlying dynamics governing bubble formation, growth, and disappearance in diverse electrolytic environments, which is essential in understanding and improving industrial processes.

5. Conclusions and perspectives

This review provides a comprehensive analysis of diverse *in-situ* characterization methods, including *in-situ* microscopy and X-ray μ-CT, and their utility in investigating the progression of physical phases, composition, and interfaces in metallurgical processes. Each of these techniques provides distinct advantages and features, enabling the examination of electrochemical reaction mechanisms in metal melting processes from diverse viewpoints and scales. *In-situ* scanning electron microscopy (SEM) enables the examination of alterations in the surface morphology of electrodes and slag. However, SEM has limitations in terms of its capability to visualize internal changes occurring within the electrode. By contrast, the utilization of *in-situ* transmission electron microscopy helps achieve an atomic-level spatial resolution, hence enabling the precise analysis of interior crystalline structures and chemical states. Nevertheless, the persistent exposure of a high-energy electron beam can affect the electrochemical reaction mechanism. The utilization of *in-situ* X-ray technology, characterized by its notable capacity for deep penetration, enables the scanning of electrodes to acquire valuable insights into their physical phase through XRD analysis, as well as their 3D structure via X-ray μ-CT. Raman spectroscopy is a technique that utilizes the phenomenon of inelastic scattering of laser light to identify changes in the composition and structure of a given material [90]. This review notes that any *in-situ* characterization technique has inherent limitations and is best suited for specific applications. To effectively utilize *in-situ* characterization in industrial production, the temperature range of these methods needs to be expanded, and techniques that can monitor reactions in real industrial settings rather than just in controlled laboratory environments need to be created. A complete and systematic investigation of metallurgical processes often necessitates the utilization of a combination of approaches, depending on the unique research requirements. The continuous advancement of technology is expected to improve the operating temperature, time resolution, energy resolution, and spatial resolution of these techniques, hence resulting in more reliable data acquisition and processing systems. Future progress of *in-situ* characterization techniques is anticipated to facilitate the capability to observe electrodes, molten salts, and their interfaces in real time throughout the process of electrochemical metallurgy electrolysis [91]. The present study aims to establish a correlation between the evolutionary patterns of microstructures, components, elements, and chemical state distributions and the real-time electrochemical signals. This correlation will serve as a robust basis for conducting data analysis to effectively handle the intricate nature of electrode interfaces. This study aims to propose a novel methodology for the observation and optimization of electrochemical processes, with a focus on enhancing their efficiency and stability. The primary objective of this endeavor is to build a robust electrolysis technology and provide a novel approach for data collection and analysis in the field of electrochemistry.

This review emphasizes the significance of *in-situ* characterization approaches in the advancement of our comprehension of metallurgical processes, specifically in the context of electrochemical metallurgy electrolysis. The utilization of these approaches is of significance in facilitating the real-time monitoring and study of the dynamic alterations occurring at electrodes, within molten salts, and at the interfaces between them. Each technique has distinct strengths and limits, rendering them appropriate for certain facets of metallurgical study [92–93]. For example, *in-situ* microscopy provides detailed insights into surface morphology, whereas X-ray-based methods reveal internal structures and phase changes. The choice of technique or combination of techniques hinges on the research objectives. A multifaceted approach often yields the most comprehensive understanding, as it enables colleagues in the industry to cross-verify findings and build a more complete picture of the electrochemical processes at play. Technological advancements are expected to push the boundaries of these techniques further, enhancing their resolution and sensitivity. Improvements in working temperature ranges, time resolution, energy resolution, and spatial resolution are on the horizon, which will significantly bolster data acquisition and analysis capabilities [94–95]. The future of *in-situ* characterization looks prom-

ising, with potential developments enabling systematic real-time monitoring of metal melting processes. The advancement described is of utmost importance in addressing the difficulties presented by the intricate and fluctuating electrode interfaces, commonly referred to as the "black box" phenomenon, and plays a vital role in guaranteeing the consistent functionality of electrochemical processes. By linking microstructural evolution, compositional changes, and electrochemical signals, colleagues in the industry can gain insights into the fundamental mechanisms governing electrolysis. This knowledge is key to developing new methods for electrochemistry visualization, optimizing process efficiency, and establishing stable electrolysis technologies. In essence, the continuous improvement of *in-situ* characterization techniques is set to revolutionize our ability to visualize electrochemical processes, master their efficient and stable operation, and provide novel methods for data acquisition and analysis, which will not only enhance our fundamental understanding but also drive innovation in electrochemical process design and control.

Despite the existence of notable obstacles in implementing multiscale *in-situ* characterization methods in industrial production, such as the integration of characterization devices with large-scale production equipment and the energy consumption associated with *in-situ* characterization devices, the potential benefits should not be overlooked. The *in-situ* characterization method has demonstrated considerable potential and satisfies the fundamental requirements for utilization in intricate high-temperature situations. However, the endeavor necessitates a protracted period of comprehensive investigation and advancement. Therefore, additional research and development on high-temperature *in-situ* characterization methods and approaches need to be conducted to facilitate their extensive utilization in industrial production.

Acknowledgement

This work was financially supported by the National Key R&D Program of China (No. 2022YFC2906100).

Conflict of Interest

Shuqiang Jiao is a vice editor-in-chief for this journal and was not involved in the editorial review or the decision to publish this article. The authors have no competing interests to declare that are relevant to the content of this article.

References

[1] G.Z. Chen, D.J. Fray, and T.W. Farthing, Direct electrochemical reduction of titanium dioxide to titanium in molten calcium chloride, *Nature*, 407(2000), p. 361.

[2] X.L. Zou, L. Ji, J.B. Ge, D.R. Sadoway, E.T. Yu, and A.J. Bard, Electrodeposition of crystalline silicon films from silicon dioxide for low-cost photovoltaic applications, *Nat. Commun.*, 10(2019), art. No. 5772.

[3] H.Y. Yin, B. Chung, F. Chen, T. Ouchi, J. Zhao, N. Tanaka, and D.R. Sadoway, Faradaically selective membrane for liquid metal displacement batteries, *Nat. Energy*, 3(2018), p. 127.

[4] K.L. Wang, K. Jiang, B. Chung, *et al*., Lithium–antimony–lead liquid metal battery for grid-level energy storage, *Nature*, 514(2014), p. 348.

[5] P. Sarfo, A. Das, and C. Young, Extraction and optimization of neodymium from molten fluoride electrolysis, *Sep. Purif. Technol.*, 256(2021), art. No. 117770.

[6] H.D. Jiao, W.L. Song, H.S. Chen, M.Y. Wang, S.Q. Jiao, and D.N. Fang, Sustainable recycling of titanium scraps and purity titanium production via molten salt electrolysis, *J. Cleaner Prod.*, 261(2020), art. No. 121314.

[7] H.Y. Yin, X.H. Mao, D.Y. Tang, *et al*., Capture and electrochemical conversion of CO_2 to value-added carbon and oxygen by molten salt electrolysis, *Energy Environ. Sci.*, 6(2013), No. 5, p. 1538.

[8] D.R. MacFarlane, M. Forsyth, P.C. Howlett, *et al*., Ionic liquids and their solid-state analogues as materials for energy generation and storage, *Nat. Rev. Mater.*, 1(2016), No. 2, art. No. 15005.

[9] M.E. Wagner and A. Allanore, Electrochemical separation of Ag_2S and Cu_2S from molten sulfide electrolyte, *J. Electrochem. Soc.*, 169(2022), No. 6, art. No. 063511.

[10] S.Q. Jiao, H.D. Jiao, W.L. Song, M.Y. Wang, and J.G. Tu, A review on liquid metals as cathodes for molten salt/oxide electrolysis, *Int. J. Miner. Metall. Mater.*, 27(2020), No. 12, p. 1588.

[11] K. Sun, J.H. Wu, and Y.Y. Ma, The state-of-the-art of nonferrous extractive metallurgy and its development trend, *Nonferrous Met.*, 4(1999) , p. 76.

[12] R. Yuan, H.D. Jiao, H.M. Zhu, D.N. Fang, and S.Q. Jiao, *In situ* characterization techniques and methodologies for high-temperature electrochemistry, *Chem*, 9(2023), No. 9, p. 2481.

[13] S.Q. Jiao, M.Y. Wang, and W.L. Song, Editorial for special issue on high-temperature molten salt chemistry and technology, *Int. J. Miner. Metall. Mater.*, 27(2020), No. 12, p. 1569.

[14] Y. Ito, A bright future for molten salts in science and technology, *Electrochemistry*, 67(1999), No. 6, art. No. 528.

[15] W. Xiao, J. Zhou, L. Yu, D.H. Wang, and X.W.D. Lou, Electrolytic formation of crystalline silicon/germanium alloy nanotubes and hollow particles with enhanced lithium-storage properties, *Angew. Chem. Int. Ed.*, 55(2016), No. 26, p. 7427.

[16] Y.F. Chen, B. Gao, M.Y. Wang, X. Xiao, A.J. Lv, S.Q. Jiao, and P.K. Chu, Dual-phase MoC−Mo_2C nanosheets prepared by molten salt electrochemical conversion of CO_2 as excellent electrocatalysts for the hydrogen evolution reaction, *Nano Energy*, 90(2021), art. No. 106533.

[17] T. Wang, Y.R. Zhang, B.T. Huang, *et al*., Enhancing oxygen reduction electrocatalysis by tuning interfacial hydrogen bonds, *Nat. Catal.*, 4(2021), No. 9, p. 753.

[18] D. Prasai, J.C. Tuberquia, R.R. Harl, G.K. Jennings, and K.I. Bolotin, Graphene: Corrosion-inhibiting coating, *ACS Nano*, 6(2012), No. 2, p. 1102.

[19] W. Xiao and D.H. Wang, The electrochemical reduction processes of solid compounds in high temperature molten salts, *Chem. Soc. Rev.*, 43(2014), No. 10, p. 3215.

[20] K. Carlson, L. Gardner, J. Moon, B. Riley, J. Amoroso, and D. Chidambaram, Molten salt reactors and electrochemical reprocessing: Synthesis and chemical durability of potential waste forms for metal and salt waste streams, *Int. Mater. Rev.*, 66(2021), No. 5, p. 339.

[21] Z.Y. Pang, X.L. Zou, S.S. Li, W. Tang, Q. Xu, and X.G. Lu, Molten salt electrochemical synthesis of ternary carbide Ti_3AlC_2 from titanium-rich slag, *Adv. Eng. Mater.*, 22(2020), No. 5, art. No. 1901300.

[22] X. Lu, Z.Y. Zhang, T. Hiraki, O. Takeda, H.M. Zhu, K. Matsubae, and T. Nagasaka, A solid-state electrolysis process for upcycling aluminium scrap, *Nature*, 606(2022), p. 511.

[23] A. Allanore, L. Yin, and D.R. Sadoway, A new anode material

for oxygen evolution in molten oxide electrolysis, *Nature*, 497(2013), p. 353.
[24] J.A. Hoffman, M.H. Hecht, D. Rapp, *et al*., Mars Oxygen ISRU Experiment (MOXIE)-Preparing for human Mars exploration, *Sci. Adv.*, 8(2022), No. 35, art. No. eabp8636.
[25] J.K. Li and J.L. Gong, Operando characterization techniques for electrocatalysis, *Energy Environ. Sci.*, 13(2020), No. 11, p. 3748.
[26] Q. Meyer, Y. Zeng, and C. Zhao, *In situ* and operando characterization of proton exchange membrane fuel cells, *Adv Mater*, 31(2019), No. 40, art. No. e1901900.
[27] A.D. Handoko, F.X. Wei, Jenndy, B.S. Yeo, and Z.W. Seh, Understanding heterogeneous electrocatalytic carbon dioxide reduction through operando techniques, *Nat. Catal.*, 1(2018), p. 922.
[28] Z.F. Lin, P.L. Taberna, and P. Simon, Advanced analytical techniques to characterize materials for electrochemical capacitors, *Curr. Opin. Electrochem.*, 9(2018), p. 18.
[29] X. Liu, Y. Tong, Y. Wu, J. Zheng, Y. Sun, and H. Li, In-depth mechanism understanding for potassium-ion batteries by electroanalytical methods and advanced *in situ* characterization techniques, *Small Meth.*, 5(2021), No. 12, art. No. e2101130.
[30] R. Yuan, C. Lv, H.L. Wan, *et al*., Electrochemical behavior of vanadium ions in molten LiCl−KCl, *J. Electroanal. Chem.*, 891(2021), art. No. 115259.
[31] B.W. Deng, J.J. Tang, X.H. Mao, Y.Q. Song, H. Zhu, W. Xiao, and D.H. Wang, Kinetic and thermodynamic characterization of enhanced carbon dioxide absorption process with lithium oxide-containing ternary molten carbonate, *Environ. Sci. Technol.*, 50(2016), No. 19, p. 10588.
[32] M.R. Rowles, N.V.Y. Scarlett, I.C. Madsen, and K. McGregor, Characterization of rutile passivation layers formed on Magnéli-phase titanium oxide inert anodes, *J. Appl. Crystallogr.*, 44(2011), No. 4, p. 853.
[33] B. Feng, P. Wu, and Y.L. Li, *In situ* XRD analysis of reduction mechanism of Fe_2O_3, *Nat. Gas Chem. Ind.*, 46(2021), No. 1, p. 66.
[34] T.Y. Guo, S.Y. Liu, M. Qing, *et al*., *In situ* XRD study of the effect of H_2O on Fe_5C_2 phase and Fischer-Tropsch performance, *J. Fuel Chem. Technol.*, 48(2020), No. 1, p. 75.
[35] Y.L. Xu, M.B. Xu, and S.J. Yang, Application of X-ray powder diffraction in phase analysis of inorganic synthesis, *J. Hubei Normal Univ.*, 33(2013), No. 4, p. 40.
[36] M.L. Wang, G.H. Shi, X.H. Zhang, Z.Y. Yang, and Y.M. Xing, Experimental study on high-temperature phase transformation of calcite, *Spectrosc. Spect. Anal.*, 43(2023), No. 4, p. 1205.
[37] S.H. Tong, Y. Li, M.W. Yan, P. Jiang, J.J. Ma, and D.D. Yue, *In situ* reaction mechanism of MgAlON in Al–Al_2O_3–MgO composites at 1700°C under flowing N2, *Int. J. Miner. Metall. Mater.*, 24(2017), No. 9, p. 1061.
[38] M. Clancy, M.J. Styles, C.J. Bettles, N. Birbilis, J.A. Kimpton, and N.A.S. Webster, *In situ* XRD investigation of the evolution of surface layers on Pb-alloy anodes, *Powder Diffr.*, 32(2017), No. S2, p. S54.
[39] A. Rasooli, M. Divandari, H.R. Shahverdi, and M. Ali Boutorabi, Kinetics and mechanism of titanium hydride powder and aluminum melt reaction, *Int. J. Miner. Metall. Mater.*, 19(2012), No. 2, p. 165.
[40] F. Nikkhou, F. Xia, X.Z. Yao, I.A. Adegoke, Q.F. Gu, and J.A. Kimpton, A flow-through reaction cell for studying minerals leaching by *In-situ* synchrotron powder X-ray diffraction, *Minerals*, 10(2020), No. 11, art. No. 990.
[41] A. Mukherjee, J. Van Dyck, B. Blanpain, and M.X. Guo, CSLM study on the interaction of Nd_2O_3 with $CaCl_2$ and CaF_2–LiF molten melts, *J. Mater. Sci.*, 52(2017), No. 3, p. 1717.
[42] Y.M. Lee, J.K. Yang, D.J. Min, and J.H. Park, Mechanism of MgO dissolution in MgF_2–CaF_2–MF (M=Li or Na) melts: Kinetic analysis via *in situ* high temperature confocal scanning laser microscopy (HT-CSLM), *Ceram. Int.*, 45(2019), No. 16, p. 20251.
[43] X.J. Zhao, Z.N. Yang, and F.C. Zhang, *In situ* observation of the effect of AlN particles on bainitic transformation in a carbide-free medium carbon steel, *Int. J. Miner. Metall. Mater.*, 27(2020), No. 5, p. 620.
[44] N. Fuchs and C. Bernhard, Potential and limitations of direct austenite grain growth measurement by means of HT-LSCM, *Mater. Today Commun.*, 28(2021), art. No. 102468.
[45] H. Liu, W.F. Li, C.Y. Ren, L.F. Zhang, and Y. Ren, Inclusion evolution in Al-killed Ca-treated steels at heat treatment temperature *in situ* observed using confocal scanning laser microscope, *Metall. Mater. Trans. B*, 53(2022), No. 3, p. 1323.
[46] C.Y. Ren, C.D. Huang, L.F. Zhang, and Y. Ren, *In situ* observation of the dissolution kinetics of Al_2O_3 particles in CaO–Al_2O_3–SiO_2 slags using laser confocal scanning microscopy, *Int. J. Miner. Metall. Mater.*, 30(2023), No. 2, p. 345.
[47] H. Yao, Q. Ren, W. Yang, and L.F. Zhang, *In situ* observation and prediction of the transformation of acicular ferrites in Ti-containing HLSA steel, *Metall. Mater. Trans. B*, 53(2022), No. 3, p. 1827.
[48] A. Ale, V. Ermolayev, E. Herzog, C. Cohrs, M.H. de Angelis, and V. Ntziachristos, FMT–XCT: *In vivo* animal studies with hybrid fluorescence molecular tomography–X-ray computed tomography, *Nat. Meth.*, 9(2012), p. 615.
[49] X. Zhang, C. Wang, K. He, *et al*., Transport performance of molten salt electrolyte in a fractal porous FeS_2 electrode: Mesoscale modeling and experimental characterization, *ACS Appl. Energy Mater.*, 4(2021), No. 12, p. 14363.
[50] Y.T. Jee, M. Park, S. Cho, and J.I. Yun, Selective morphological analysis of cerium metal in electrodeposit recovered from molten LiCl–KCl eutectic by radiography and computed tomography, *Sci. Rep.*, 9(2019), art. No. 1346.
[51] X.K. Lu, A. Bertei, D.P. Finegan, *et al*., 3D microstructure design of lithium-ion battery electrodes assisted by X-ray nano-computed tomography and modelling, *Nat. Commun.*, 11(2020), art. No. 2079.
[52] T.M.M. Heenan, A.V. Llewellyn, A.S. Leach, *et al*., Resolving Li-ion battery electrode particles using rapid lab-based X-ray nano-computed tomography for high-throughput quantification, *Adv Sci Weinh*, 7(2020), No. 12, art. No. 2000362.
[53] X.Y. Liu, A. Ronne, L.C. Yu, *et al*., Formation of three-dimensional bicontinuous structures via molten salt dealloying studied in real-time by *in situ* synchrotron X-ray nano-tomography, *Nat. Commun.*, 12(2021), No. 1, art. No. 3441.
[54] H. Lusic and M.W. Grinstaff, X-ray-computed tomography contrast agents, *Chem Rev*, 113(2013), No. 3, p. 1641.
[55] Z.Y. Ding, N.F. Zhang, L. Yu, W.Q. Lu, J.G. Li, and Q.D. Hu, Recent progress in metallurgical bonding mechanisms at the liquid/solid interface of dissimilar metals investigated via *in situ* X-ray imaging technologies, *Acta Metall. Sin. Engl. Lett.*, 34(2021), No. 2, p. 145.
[56] H. Jiao, Z. Qu, S. Jiao, *et al*., A 4D X-ray computer microtomography for high-temperature electrochemistry, *Sci. Adv.*, 8(2022), No. 6, art. No. eabm5678.
[57] S.W. Hudson, J. Craparo, R. De Saro, and D. Apelian, Applications of laser-induced breakdown spectroscopy (LIBS) in molten metal processing, *Metall. Mater. Trans. B*, 48(2017), No. 5, p. 2731.
[58] F.Z. Dong, X.L. Chen, Q. Wang, *et al*., Recent progress on the application of LIBS for metallurgical online analysis in China, *Front. Phys.*, 7(2012), No. 6, p. 679.
[59] L.X. Sun, H.B. Yu, Z.B. Cong, *et al*., Applications of laser-induced breakdown spectroscopy in the aluminum electrolysis industry, *Spectrochim. Acta*, 142(2018), p. 29.
[60] J. Gruber, J. Heitz, H. Strasser, D. Bäuerle, and N. Ramaseder,

Rapid *in situ* analysis of liquid steel by laser-induced breakdown spectroscopy, *Spectrochim. Acta*, 56(2001), No. 6, p. 685.
[61] J. Gruber, J. Heitz, N. Arnold, *et al.*, *In situ* analysis of metal melts in metallurgic vacuum devices by laser-induced breakdown spectroscopy, *Appl. Spectrosc.*, 58(2004), No. 4, p. 457.
[62] L. Peter, V. Sturm, and R. Noll, Liquid steel analysis with laser-induced breakdown spectrometry in the vacuum ultraviolet, *Appl. Opt.*, 42(2003), No. 30, p. 6199.
[63] V. Sturm, H.U. Schmitz, T. Reuter, R. Fleige, and R. Noll, Fast vacuum slag analysis in a steel works by laser-induced breakdown spectroscopy, *Spectrochim. Acta Part B*, 63(2008), No. 10, p. 1167.
[64] P. Zhang, L. Sun, H. Yu, P. Zeng, L. Qi, and Y. Xin, An image auxiliary method for quantitative analysis of laser-induced breakdown spectroscopy, *Anal. Chem.*, 90(2018), No. 7, p. 4686.
[65] F. Gao, X.D. Tian, J.S. Lin, J.C. Dong, X.M. Lin, and J.F. Li, *In situ* Raman, FTIR, and XRD spectroscopic studies in fuel cells and rechargeable batteries, *Nano Res.*, 16(2023), No. 4, p. 4855.
[66] X. Li, Z.Y. Pang, W. Tang, *et al.*, Electrodeposition of Si films from SiO_2 in molten $CaCl_2$–CaO: The dissolution-electrodeposition mechanism and its epitaxial growth behavior, *Metall. Mater. Trans. B*, 53(2022), No. 5, p. 2800.
[67] W.T. Zhou, J.S. Zhang, and Y.F. Wang, Review—Modeling electrochemical processing for applications in pyroprocessing, *J. Electrochem. Soc.*, 165(2018), No. 13, p. E712.
[68] J.Y. Yu, C.Y. Liu, X.W. Hu, T. Yuan, Y.F. Zhang, Z.W. Wang, and W.R. Ji, Preparation of aAu SERS substrate and its application in the *in situ* Raman spectroelectrochemistry study of Li_2CO_3–K_2CO_3 molten salt, *Int. J. Electrochem. Sci.*, 16(2021), No. 11, art. No. 211131.
[69] I. Novoselova, S.V. Kuleshov, A.A. Omel'chuk, V.V. Soloviev, and N.V. Solovyova, Cationic catalysis during the discharge of carbonate anions in molten salts, *ECS Trans.*, 98(2020), No. 10, p. 317.
[70] N. Ma, J.L. You, L.M. Lu, Y.F. Xie, and S.M. Wan, Quantitative analysis on the microstructure of molten binary KF-AlF_3 system by *in situ* Raman spectroscopy assisted with first principles method, *J. Raman Spectrosc.*, 51(2020), No. 1, p. 187.
[71] L.J. Chen, X. Cheng, C.J. Lin, and C.M. Huang, *In-situ* Raman spectroscopic studies on the oxide species in molten Li/K_2CO_3, *Electrochim. Acta*, 47(2002), No. 9, p. 1475.
[72] N. Ma, J.L. You, L.M. Lu, J. Wang, M. Wang, and S.M. Wan, Micro-structure studies of the molten binary K_3AlF_6–Al_2O_3 system by *in situ* high temperature Raman spectroscopy and theoretical simulation, *Inorg. Chem. Front.*, 5(2018), No. 8, p. 1861.
[73] X.W. Hu, W.T. Deng, Z.N. Shi, Z.X. Wang, B.L. Gao, and Z.W. Wang, Solubility of CO_2 in molten Li_2O–LiCl system: A Raman spectroscopy study, *J. Chem. Eng. Data*, 64(2019), No. 1, p. 202.
[74] R. Zhang, Y. Wang, X. Zhao, J.X. Jia, C.J. Liu, and Y. Min, Structure and viscosity of molten CaO–SiO_2–Fe_xO slag during the early period of basic oxygen steelmaking, *Metall. Mater. Trans. B*, 51(2020), No. 5, p. 2021.
[75] H.D. Jiao, J.L. An, Y.Z. Jia, *et al.*, Operando probing and adjusting of the complicated electrode process of multivalent metals at extreme temperature, *Proc. Natl. Acad. Sci. U.S.A.*, 120(2023), No. 28, art. No. e2301780120.
[76] Y.Y. Liu, Y.L. Song, H. Ai, *et al.*, Corrosion of Cr in molten salts with different fluoroacidity in the presence of CrF_3, *Corros. Sci.*, 169(2020), art. No. 108636.
[77] B.R. Sundheim and J. Greenberg, Absorption spectra of molten salts, *J. Chem. Phys.*, 28(1958), No. 3, p. 439.
[78] C. Hardacre, Application of EXAFS to molten salts and ionic liquid technology, *Annu. Rev. Mater. Res.*, 35(2005), No. 5, p. 29.
[79] E.D. Crozier, N. Alberding, and B.R. Sundheim, EXAFS study of bromomanganate ions in molten salts, *J. Chem. Phys.*, 79(1983), No. 2, p. 939.
[80] A. Di Cicco, M. Taglienti, M. Minicucci, and A. Filipponi, Short-range structure of solid and liquid AgBr determined by multiple-edge X-ray absorption spectroscopy, *Phys. Rev. B*, 62(2000), No. 18, p. 12001.
[81] T.J. Kim, A. Uehara, T. Nagai, T. Fujii, and H. Yamana, Quantitative analysis of Eu^{2+} and Eu^{3+} in LiCl–KCl eutectic melt by spectrophotometry and electrochemistry, *J. Nucl. Mater.*, 409(2011), No. 3, p. 188.
[82] B.Y. Kim and J.I. Yun, Reduction of trivalent europium in molten LiCl-KCl eutectic observed by *In-situ* laser spectroscopic techniques, *ECS Electrochem. Lett.*, 2(2013), No. 11, p. H54.
[83] C. Bessada and E.M. Anghel, ^{11}B, ^{23}Na, ^{27}Al, and ^{19}F NMR study of solid and molten Na_3AlF_6–$Na_2B_4O_7$, *Inorg. Chem.*, 42(2003), No. 12, p. 3884.
[84] Y.F. Cui, Y. He, W.T. Yu, W.X. Shang, Y.Y. Ma, and P. Tan, *In-situ* observation of the Zn electrodeposition on the planar electrode in the alkaline electrolytes with different viscosities, *Electrochim. Acta*, 418(2022), art. No. 140344.
[85] H.D. Jiao, M.J. Liu, Y. Gao, J.X. Song, and S.Q. Jiao, Dynamic evolution of high-temperature molten salt electrolysis of titanium under different operational conditions, *Inorg. Chem. Front.*, 10(2023), No. 2, p. 529.
[86] S. Fortin, M. Gerhardt, and A.J. Gesing, Physical modelling of bubble behaviour and gas release from aluminum reduction cell anodes, [in] G. Bearne, M. Dupuis, and G. Tarcy, eds., *Essential Readings in Light Metals*, Springer, Cham, 2016, p. 385.
[87] Z.B. Zhao, Z.W. Wang, B.L. Gao, Y.Q. Feng, Z.N. Shi, and X.W. Hu, Anodic bubble behavior and voltage drop in a laboratory transparent aluminum electrolytic cell, *Metall. Mater. Trans. B*, 47(2016), No. 3, p. 1962.
[88] T. Utigard, J. Toguri, and S. Ip, Direct observation of the anode effect by radiography, [in] G. Bearne, M. Dupuis, G. Tarcy, eds., *Essential Readings in Light Metals*, Springer, Cham, 2016, p. 167.
[89] Z.Y. Ding, Q.D. Hu, W.Q. Lu, *et al.*, *In-situ* study on hydrogen bubble evolution in the liquid Al/solid Ni interconnection by synchrotron radiation X-ray radiography, *J. Mater. Sci. Technol.*, 35(2019), No. 7, p. 1388.
[90] S.S. Liu, S.L. Li, C.H. Liu, J.L. He, and J.X. Song, Effect of fluoride ions on coordination structure of titanium in molten NaCl-KCl, *Int. J. Miner. Metall. Mater.*, 30(2023), No. 5, p. 868.
[91] M. Yang, R.Y. Bi, J.Y. Wang, R.B. Yu, and D. Wang, Decoding lithium batteries through advanced *in situ* characterization techniques, *Int. J. Miner. Metall. Mater.*, 29(2022), No. 5, p. 965.
[92] X. Song, S.L. Li, S.S. Liu, Y. Fan, J.L. He, and J.X. Song, Coordination states of metal ions in molten salts and their characterization methods, *Int. J. Miner. Metall. Mater.*, 30(2023), No. 7, p. 1261.
[93] X.Q. He, H.D. Fu, and J.X. Xie, Microstructure and properties evolution of in-situ fiber-reinforced Ag–Cu–Ni–Ce alloy during deformation and heat treatment, *Int. J. Miner. Metall. Mater.*, 29(2022), No. 11, p. 2000.
[94] J.C. Li, G.X. Li, F. Qiu, *et al.*, Nucleation and growth control for iron- and phosphorus-rich phases from a modified steelmaking waste slag, *Int. J. Miner. Metall. Mater.*, 30(2023), No. 2, p. 378.
[95] B. Sun, J.T. Dai, K.K. Huang, C.H. Yang, and W.H. Gui, Smart manufacturing of nonferrous metallurgical processes: Review and perspectives, *Int. J. Miner. Metall. Mater.*, 29(2022), No. 4, p. 611.